1973

A study of the effect of internal wave induced turbulence on small scale temperature structure in shallow water.

Minard, Julian Edward.

Monterey, California. Naval Postgraduate School

A STUDY OF THE EFFECT OF INTERNAL WAVE INDUCED TURBULENCE ON SMALL SCALE TEMPERATURE STRUCTURE IN SHALLOW WATER

Julian Edward Minard

NAVAL POSTGRADUATE SCHOOL
Monterey, California

THESIS

A STUDY OF THE EFFECT OF
INTERNAL WAVE INDUCED TURBULENCE ON
SMALL SCALE TEMPERATURE STRUCTURE
IN SHALLOW WATER

by

Julian Edward Minard

Thesis Advisor: N. Boston
E. Thornton

September 1973

Approved for public release; distribution unlimited.

A Study of the Effect of Internal Wave Induced Turbulence on Small Scale Temperature Structure in Shallow Water

by

Julian Edward Minard
Lieutenant Commander, United States Navy
A.B., Brown University, 1962

Submitted in partial fulfillment of the
requirements for the degree of

MASTER OF SCIENCE IN OCEANOGRAPHY

from the

NAVAL POSTGRADUATE SCHOOL
September 1973

ABSTRACT

Measurements of temporal and spatial scale sizes of small scale temperature fluctuations were made in 19 meters of water from the NUC Oceanographic Research Tower off San Diego, California. Horizontal and vertical measurements were made using a two meter straight line array of seven thermistors. In addition to temperature, waves and orthogonal water particle velocities (turbulence) were measured simultaneously. Internal waves were found on two of five runs.

Average correlation length and time computed for the horizontal array runs without internal waves were 118 cm (standard deviation 21.5 cm) and 10 seconds (standard deviation 4 seconds). Measurements suggested that correlations obtained from the mixed layer were longer than those obtained at the edge of the thermocline. Internal wave induced turbulence reduced spatial and temporal scales to 33 cm and 4 seconds (standard deviation 0.7 seconds).

Vertical measurements taken in the presence of internal waves yielded spatial and temporal correlations of 38 cm and 4 seconds (standard deviation 0.7 seconds).

TABLE OF CONTENTS

LIST OF FIGURES

LIST OF TABLES

ACKNOWLEDGEMENTS

The author is greatly indebted to both Dr. Noel E. J. Boston and Dr. Edward B. Thornton for the advice and time so freely given during the conduct of this experiment. The strong points of this paper are due to their inspiration.

Valuable assistance and thoughtful comment on the data was also offered by Dr. Warren W. Denner.

Technical assistance and know-how were given by Mr. Dana Mayberry and ST1 Richard Desgrange, USN, whose interest in the experiment eased many technical problems.

The experiment was funded under the following projects:

ONR Project No. NR 083-275
ORDTASC ORD 03C-002/551-1/UF 52-552-101

I. INTRODUCTION

A. HISTORICAL

For the past two years research has been carried out at the Naval Postgraduate School Department of Oceanography to study the shallow water interactions of various oceanographic processes that occur at small scales. Prior to the conduct of this experiment in May 1973, experiments were made in October 1971 and June 1972 from the Naval Undersea Center (NUC) Oceanographic Research Tower off Mission Beach, San Diego, California. Previous experiments included the simultaneous measurements of several parameters such as surface waves, water particle velocities, and fluctuations of temperature, sound speed, sound phase, and salinity. The results of these experiments are presented for the most part in MS theses of Naval Postgraduate School students. Smith [1971], Rautman [1971], Fitzgerald [1972], and Alexander [1972] reported on sound amplitude and phase fluctuations. Bordy [1972] made wave and water particle motion measurements. Krapohl [1972] made more detailed wave and turbulence measurements. Seymour [1972] initiated work on salinity measurements which were completed by Frigge [1973]. Duchock [1972] attempted to correlate sound velocity measurements with temperature and other fluctuations. Haley [1973] re-examined the October 1971 experiment in an attempt to interrelate all parameters. Gossner [1973]

compared measured sound speed at several depths with sound speed computed from empirical equations. Whittemore [1973] made progress in relating the near surface temperature field to wave motion.

From these studies, it became apparent that a more detailed examination of the small scale temperature field was required before further progress could be made in determining the interactions of other parameters.

B. STATEMENT OF THE PROBLEM

The creation of the small scale temperature field in shallow water is a complex process and may occur at various depths in the water column. At the surface, wind stresses create waves and if the stress is sufficient to produce wave breaking (white caps), then a turbulent transfer of momentum downward will result with an attendant downward flux of any excess heat in the surface water. Wind stress will also produce surface drifts. The shears from these drifts produce a certain amount of turbulence which may also be transmitted downward. This process of surface originated turbulent mixing extends downward to a depth proportional to the wavelength of the surface waves.

The ocean bottom also exerts a stress on water moving over it due to, for instance, tidal currents. The resulting shear zone causes turbulent mixing which affects the small scale temperature field and extends upward a distance proportional to the stress exerted.

The presence of a thermocline inhibits the vertical extent of the turbulence caused by the processes described above. Since the degree of stability of the water column tends to define the degree of vertical motion, the increase in stability implied by the density gradient will reduce the vertical motion of the turbulence and thus the vertical mixing.

It is paradoxical that the thermocline, which inhibits the turbulent mixing due to surface and bottom shears, may itself be the point of creation of turbulence. Internal waves propagate along the thermocline and can lead to the creation of intense turbulence. If the water masses separated by the thermocline experience relative motion, then the shear across the thermocline will produce turbulence. This relative motion may be caused by tidal currents or wind drifts. [La Fond, 1962]

It is interesting that turbulent mixing from surface and bottom shears tends to intensify the thermocline whereas turbulence caused by internal waves or current shears tends to dissipate it. Wind induced mixing redistributes heat downward to the thermocline so the deep water becomes warmer; bottom mixing essentially redistributes heat downward away from the thermocline so the upper level becomes cooler. The gradient thus becomes stronger. The internal waves tend to weaken the gradient through complex non-linear wave interactions and make the temperature difference smaller.

The greater the shear across the thermocline, the greater the possibility of instability and turbulence. It is well known that the

intensity of the shear determines the rate of growth of an unstable disturbance in a steady, stable, parallel, shearing motion. The shear instability may be described by the local Richardson number, J(z),

$$J(z) = \frac{g/\rho_0 \; \partial\rho/\partial z}{(\partial u/\partial z)^2}$$

where g is the acceleration due to gravity, ρ_0 is the reference density, $\partial\rho/\partial z$ is the rate of density change across the thermocline, and $\partial u/\partial z$ is the velocity shear across the thermocline. When the Richardson number is less than a critical value ($J(z) < 0.25$) then turbulence is possible though not certain [Phillips, 1969]. Since the maximum shear is normally found at the crests and troughs of waves, this turbulence should be expected to occur most of the time or with greatest intensity at these points. If the thermocline is intense, the critical shear will be reached earlier than if it were diffuse; an internal wave in an intense thermocline will dissipate its energy into turbulence more quickly than one in a diffuse thermocline. The turbulent mixing resulting from the passage of an internal wave results in the reduction of the shear in the thermocline to a value less than the critical value. Creation of turbulence by this means will then presumably cease until the thermocline is again restored.

An internal wave need not be a turbulent phenomenon. If there is no turbulence being created at the thermocline, then the regenerating forces of turbulent mixing from surface and bottom shears may restore the intensity again.

The interplay between propagation of energy in an internal wave and its dissipation may be summarized in the following way. An internal wave is initiated by some process and propagates along a density gradient. The shear at the boundary increases possibly due to the wave entering shallow water and changing its form or possibly due to an increase in the intensity of the density gradient or thermocline. If this shear exceeds a critical value, then turbulence may be created, probably at the crest or trough. The resulting turbulent mixing reduces the gradient possibly below the critical value. The wave then either continues propagating with energy reduced by losses to turbulence, or, if the shear is not reduced below the critical value, the wave is entirely dissipated. Areas of density gradients reduced by the mixing of past waves will not be able to support waves of such intensity of shear.

Theoretically, then, there is a cycle between an intense thermocline with intense internal wave activity producing turbulence, and a diffuse thermocline with internal waves producing little or no turbulence.

The kinetic energy of the turbulence is eventually dissipated by entrainment. Shears at the boundaries of the turbulent eddies formed by the mixing processes described above cause the shedding of smaller eddies, among which the energy of the original eddy is distributed. The energy is cascaded through eddies of decreasing size and energy

until eventually the energy is no longer sufficient to overcome the viscous forces of the surrounding water. The remaining energy is then dissipated as heat energy.

Small scale temperature gradients may exist in a field even though all velocity gradients have been removed by viscosity because the scales at which molecular diffusion of heat becomes effective are much smaller than those at which molecular viscosity is effective. This small scale temperature field is subject to being moved about as a passive scalar riding on the water particle motion caused by surface and internal waves.

C. OBJECTIVES

An experiment was conducted in May 1973 in order to make a careful examination of the small scale temperature field in the near surface region where the influence of surface waves is felt. The principal sensors were a moveable array of thermistors, a wave gauge, and a flowmeter. The object was to verify Whittemore's suggested wave-temperature coupling mechanism.

Particular attention was given to determining time and length scales. The scales that can be resolved are determined by the characteristics of the sensors and their spatial relationships with each other. For this experiment spatial scales were determined by the minimum thermistor spacing (about eight centimeters) and by the maximum spacing (about two meters). Minimum temporal scales

depended on the response time of the thermistors (0.015 seconds). Maximum scales depended on the length of the record. A maximum scale of five percent of the record length of about 20 minutes was used for the maximum lag time in calculating correlation functions giving an upper limit of one minute period waves.

The conditions of the near surface region were fulfilled by the shallow water depth of approximately 19 meters.

The May date was chosen partly for logistic reasons but also because only moderate wave activity was expected and vertical temperature gradients would not be intense. Internal wave activity was not expected to be a major source of turbulence. Unfortunately, conditions did not occur as predicted. Wind waves and swell were small or nonexistent and internal waves dominated the temperature scale much of the time. Although these conditions detracted from the original aim of the experiment, they provided an excellent opportunity to examine small scale (turbulent) temperature fluctuations in the presence of internal waves.

This thesis presents an analysis and discussion of the data taken during the May 1973 experiment conducted from the NUC tower.

II. DESCRIPTION OF THE EXPERIMENT

A. LOCATION

The experiment was conducted from the Naval Oceanographic Research Tower operated by the Naval Undersea Center (NUC) located about one mile off Mission Beach, San Diego, California. The tower consists of four deck levels about 40 ft square each on a frame of four legs. One of the decks contains a small deck house suitable for housing electronic equipment. Vertically mounted rails from one of the lower decks run down three sides of the support frame; equipment may be mounted on these rails and lowered to any pre-selected depth. The rails on the seaward face were used for the experiment since wave action was expected to come from that direction. The tower offers stable support and ample working space. Water depth at the tower is about 18.3 m with a smooth sandy bottom. [La Fond, 1965]

B. TIME

The experiment was conducted 15 and 16 May 1973; this time of year is a time of transition between winter and summer conditions. Air and sea surface temperatures are normally in the vicinity of 16.7°C, low wind, sea, and swell activity is usual, the thermocline is not likely to be strong, and internal wave activity is not yet intense.

Actual meteorological and oceanographic environmental factors observed were:

Day 1:

air temp:	15.5°C	overcast
dew point:	13.9°C	wind: calm
RH:	84%	sea sfc: negligible wind
SST:	16.5°C	waves; swell 0.7 m from west

Day 2:

air temp:	14.4-15.5°C	overcast
dew point:	13.3-13.9°C	wind: calm
RH:	84%	sea sfc: capillary waves;
SST:	16.7°C	swell 0.6 m from west

Conditions were essentially constant over the two days except the sky cleared at the end of the last run on the second day. Nansen casts were made for all runs, results are in table I; bathythermograph and sea surface temperature measurements were made for each run with a shallow BT and a bucket thermometer. The calibration of the BT was uncertain and there was considerable hysteresis. However, an estimation of thermal gradients was made for each run; the results are in table II and figure 1.

Tidal conditions were as follows:

Day 1

1340 low	1125 ebb	1407 slack
1955 high	1729 flood	

Day 2

0917 high	0933 slack	1158 ebb
1409 low	1432 slack	1754 flood

TABLE I

RESULTS OF NANSEN CASTS

RUN NUMBER	TIME	DEPTH	SALINITY
1	1315	3 m	33.743 0/00
2	1440	8 m	33.736 0/00
3	1600	14 m	33.739 0/00
4	1730	3 m	33.738 0/00
6	1100	3 m	33.743 0/00

TABLE II

ESTIMATION OF THERMAL GRADIENTS

RUN NUMBER	TOP OF GRADIENT	INTENSITY OF GRADIENT
1	4.25 m	0.98° C/m
2	10.5 m	0.88° C/m
3	7.6 m	0.79° C/m
4	14.7 m	0.25° C/m
6	sfc	0.44° C/m

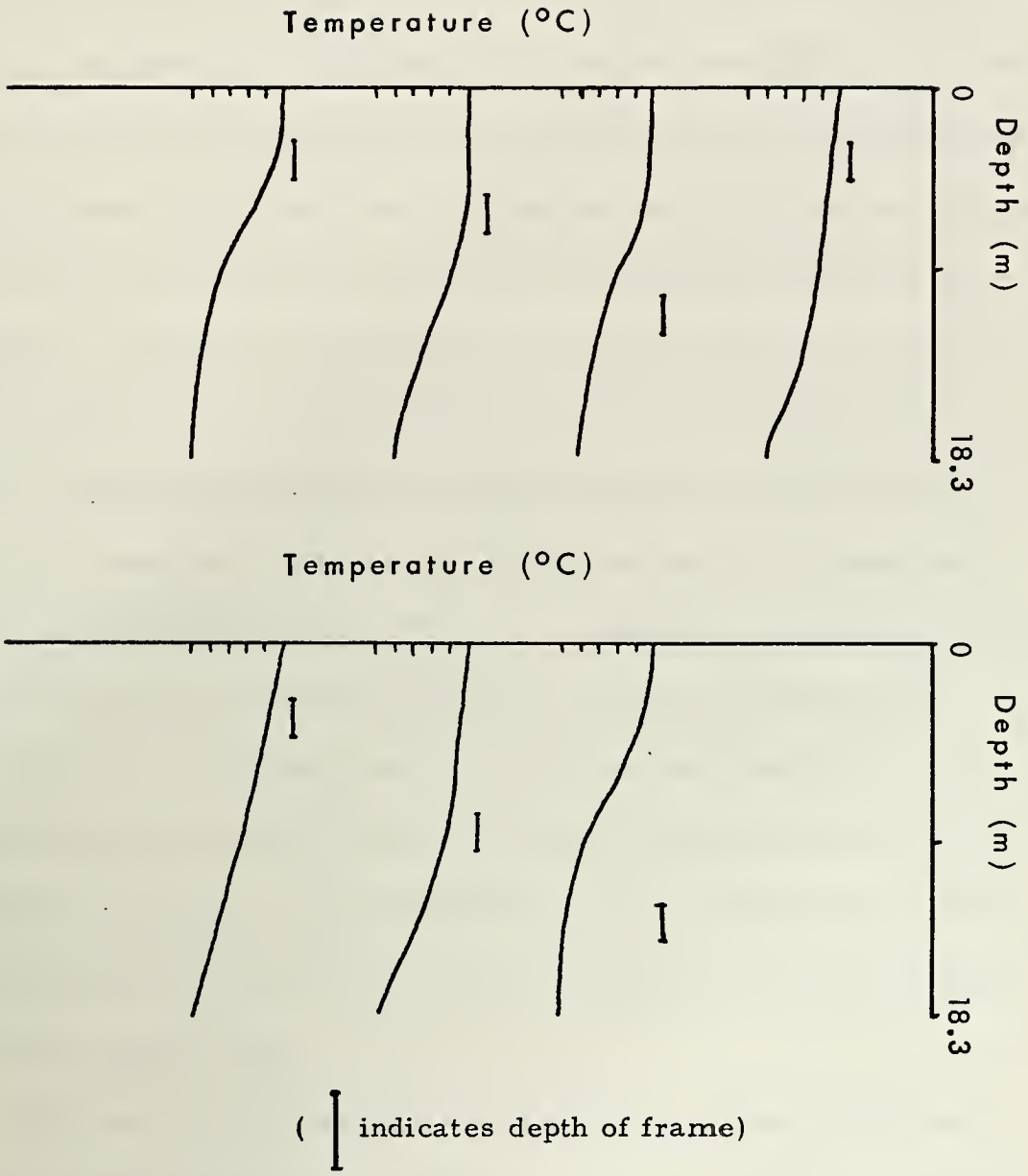

Figure 1. Bathythermograph traces

C. EQUIPMENT USED

A specially constructed 6x6x8 foot frame was mounted on the vertical rails of the seaward face of the tower by means of sliding shoes. An array of seven individually movable thermistors and a two channel electromagnetic flowmeter were mounted on the outside face of the frame. The frame was then lowered to the predetermined depth by means of an electric winch mounted on the deck at the level of the railhead. Approximate depth was determined by means of a marked cord attached to the top of the frame and payed out from the winch deck. An I-beam was mounted horizontally on the seaward face of the deck house extending over the equipment frame. A trolley ran on the underside of the beam; a Baylor wave gauge was suspended between the trolley and the top of the outside face of the equipment frame [See Fig. 2]. Since the frame was displaced horizontally as it slid down the rails due to a 5^{o} cant in the rails, the trolley was moved to keep the wave gauge vertical and directly over the flowmeter and thermistor array. Cable runs ran from all equipments to the recording room in the deck house.

The core of the experiment was seven thermistors. The thermistors were type K496 from Fenwall Electronics Inc., designed for oceanographic work. The thermistors consist of two specially aged beads in series; since there is a statistically small probability of both beads drifting or drifting in the same direction with time, they are

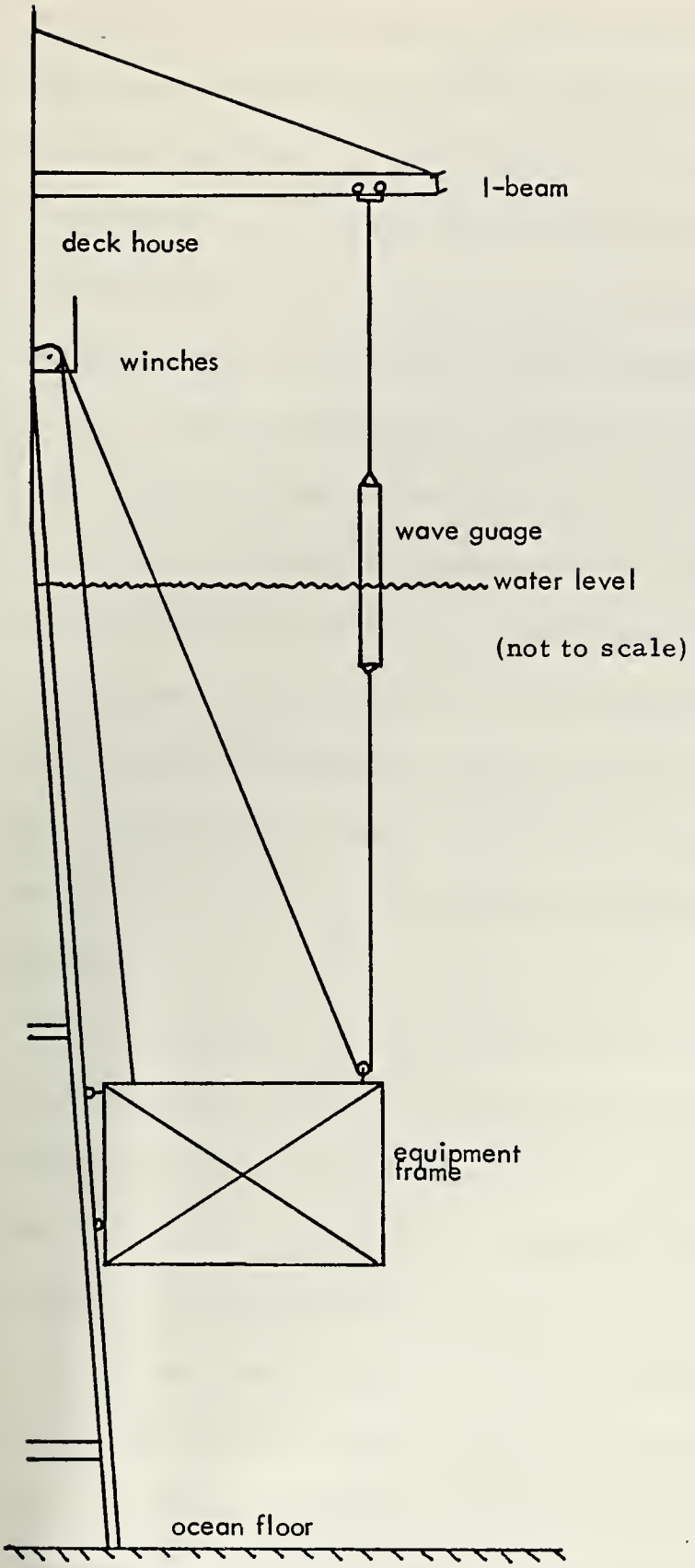

Figure 2. Layout of the Experiment

exceptionally stable and have a high repeatable accuracy. The thin glass watertight sealant around the beads allows a short response factor of 0.015 sec. High resolution is obtained from the high resistance (15 K Ω at 25°C) and a high resistance to temperature change ratio (540 K Ω /°C at 25°C). Due to low self heating, measurements accurate to the nearest 0.01°C can be obtained in seawater [Shonting, 1968]. The thermistors were mounted in a 0.3x9 cm aluminum tube with the beads extending just beyond the lip of the tube. The tube was then set in a 6 cm diameter epoxy base in which was sealed the connection between the cable run and the thermistor leads. The beads were protected in transit by a stainless steel sleeve that fitted over the tube; during the experiment they were protected from fish and seaweed by a 3 mm diameter bronze cage (Plate 1). Pipe straps were attached to the epoxy bases which allowed the thermistors to be mounted on the frame.

Associated with each thermistor was a Wheatstone bridge. Of the four legs of the bridge, two were occupied by equal fixed resistors; the balancing leg consisted of a 1 turn and a 10 turn potentiometer for coarse and fine tuning; the thermistor formed the fourth leg (Fig. 3). The bridge was constructed so that it could be balanced with the thermistor in place. A decade box could then be substituted for the thermistor and the bridge rebalanced by means of the decade box. The balancing resistance and thence the temperature of the thermistor would then be known. With the thermistor back in place,

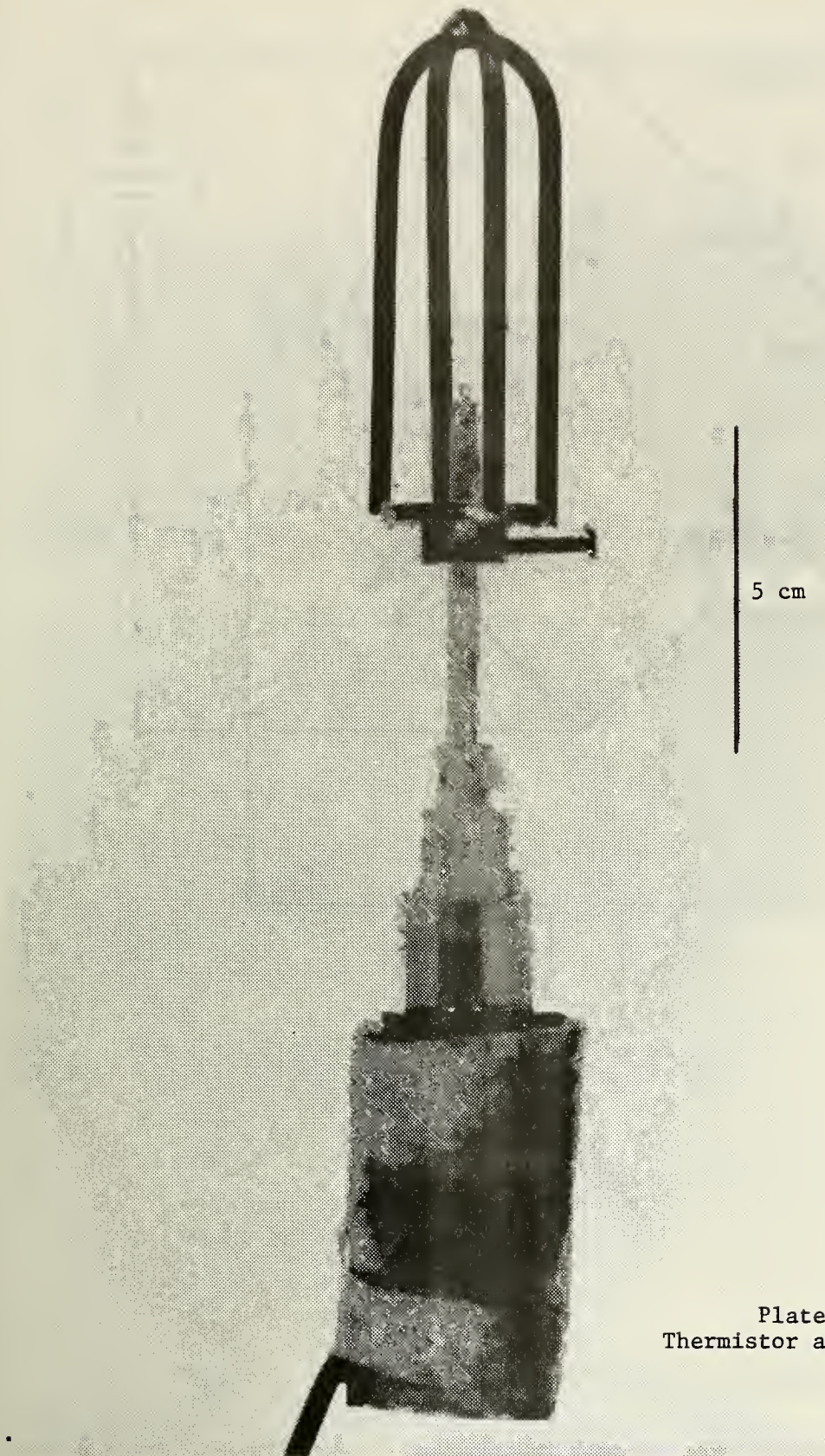

Plate 1
Thermistor and Guard

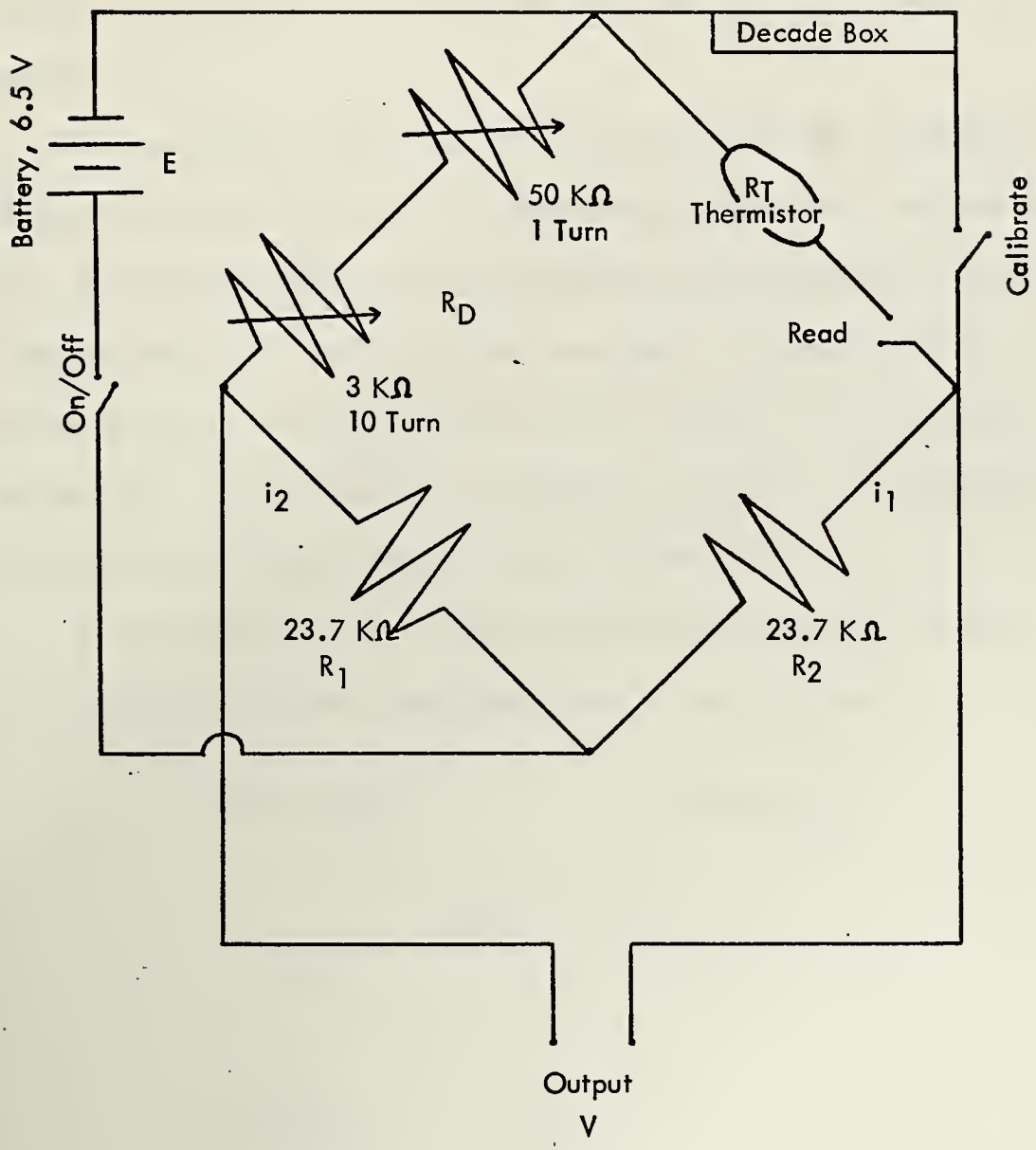

Figure 3. Circuit Diagram for Wheatstone Bridges

any voltage fluctuation across the bridge would be a function of the thermistor temperature. Power was supplied by a 6.5 V mercury battery.

The thermistors were calibrated by immersion in a fresh water bath of known temperature. The temperature of the bath was measured by a quartz thermometer which had itself been calibrated at $0^{\circ}C$ in a distilled water and ice bath. Plots were made of bridge output versus temperature for temperatures between $10^{\circ}C$ and $21^{\circ}C$ in one degree increments. The curves were sufficiently linear for a valid assumption of linearity over a range of a few degrees (Fig. 4).

The calibration factor for the individual thermistors was then determined by solution of the Wheatstone bridge equations:

$$E=(R_D+R_1)i_2 \qquad E=(R_T+R_2)i_1$$

$$V=i_2R_D - i_1R_T$$

or

$$V= \frac{R_DE}{(R_D+R_1} - \frac{R_TE}{R_T+R_2}$$

where R_T is the instantaneous resistance of the thermistor, R_D is the balance point of the bridge as determined by the decade box, R_1 and R_2 are the constant resistances, and E is the applied voltage, and V is the output of the bridge when unbalanced. The calibration factor thus determined was typically $14.9^{\circ}C/V$, (Fig. 5).

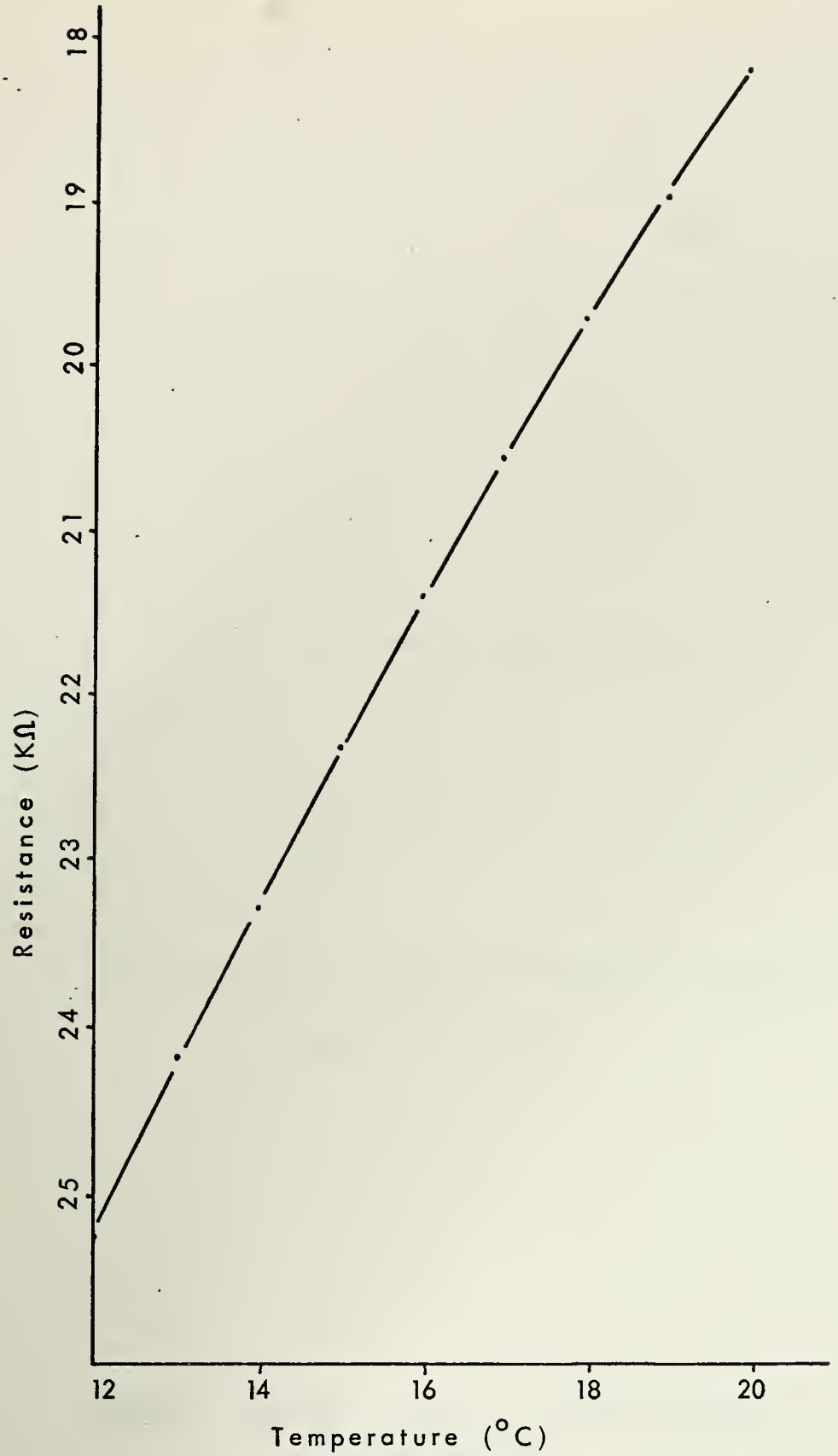

Figure 4. Typical Temperature vs Resistance Calibration Curve for Thermistors

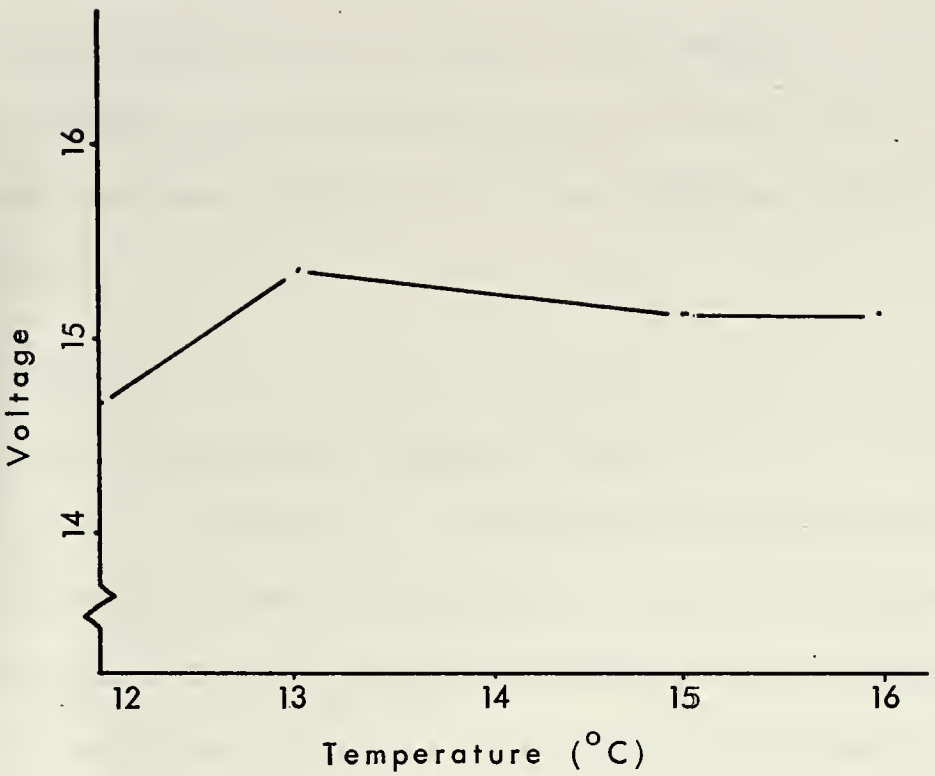

Figure 5. Calibration Factor for Wheatstone Bridge Balanced at 14°C

The Baylor wave gauge used has an accuracy of within 0.01 of wave height and a response time of less than 0.06 sec. The gauge used was 4.1 m long; its calibration factor was 7.7 m/V. The calibration curve is figure 6.

The two channel electromagnetic flowmeter was an Engineering Physics Company Water Current Meter model EMCM3B. The accuracy is to within 0.015 m/sec and has a flat response out to at least 0.5 seconds. The calibration factor was 0.541 m/sec/V. A complete description of this flow meter and calibration is given by Steer [1972].

D. RECORDING

All signals except those from the thermistors were recorded directly from the instruments. The Wheatstone bridges had to be balanced with the thermistors in the ocean during the procedures described for calibration. Voltage fluctuations caused by the temperature fluctuations in the ocean were never serious enough to prevent balancing the bridges.

Since the thermistor signals were very small (on the order of millivolts), they had to be amplified before being recorded. Seven identical amplifiers were not available, so three Preston 8300XWB and four Hewlett-Packard 2470B amplifiers were used. Unfortunately, the only gain setting they had in common was x10. For some runs in

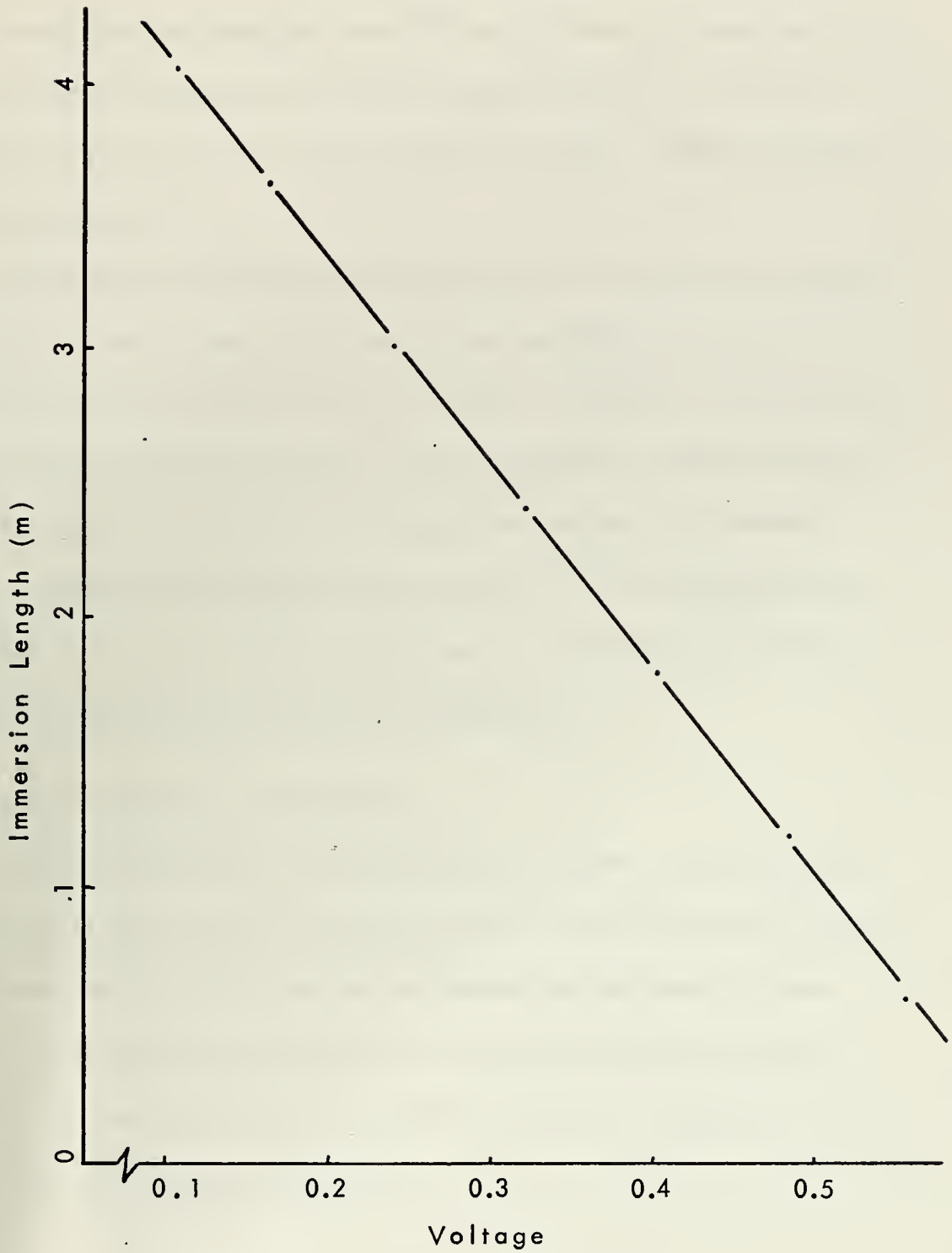

Figure 6. Calibration Curve for Baylor Wave Gauge

water with little thermal activity a higher gain setting could be used: x30 on the Preston amplifiers and x50 on the Hewlett-Packards. In the presence of internal waves when temperature excursions were relatively great, the lower gain setting was used to avoid overdriving the tape recorder.

The Preston amplifiers were equipped with a filter; consequently, on the first day channels with the Preston amplifiers were filtered at 10 Hz low pass to filter out any 60 Hz noise. However, on the second day, the filters were not used in order not to phase shift the signals.

All signals were then recorded simultaneously on a Sangamo 3562 14 channel FM magnetic tape recorder. Full scale deflection was set at $\pm$ 1 V rms. Tape speed used was 1 7/8 ips; this allowed maximum speedup (to 60 ips) during playback.

E. EXPERIMENTAL PROCEDURE

Equipment set up for the two days was similar in most respects. On the first day the thermistor array was vertical as shown in figure 7. On the second day the array was horizontal for the first two runs (Fig. 8), then for the last three runs, thermistor one was moved below the remainder of the horizontal array to give some indication of vertical temperature gradient.

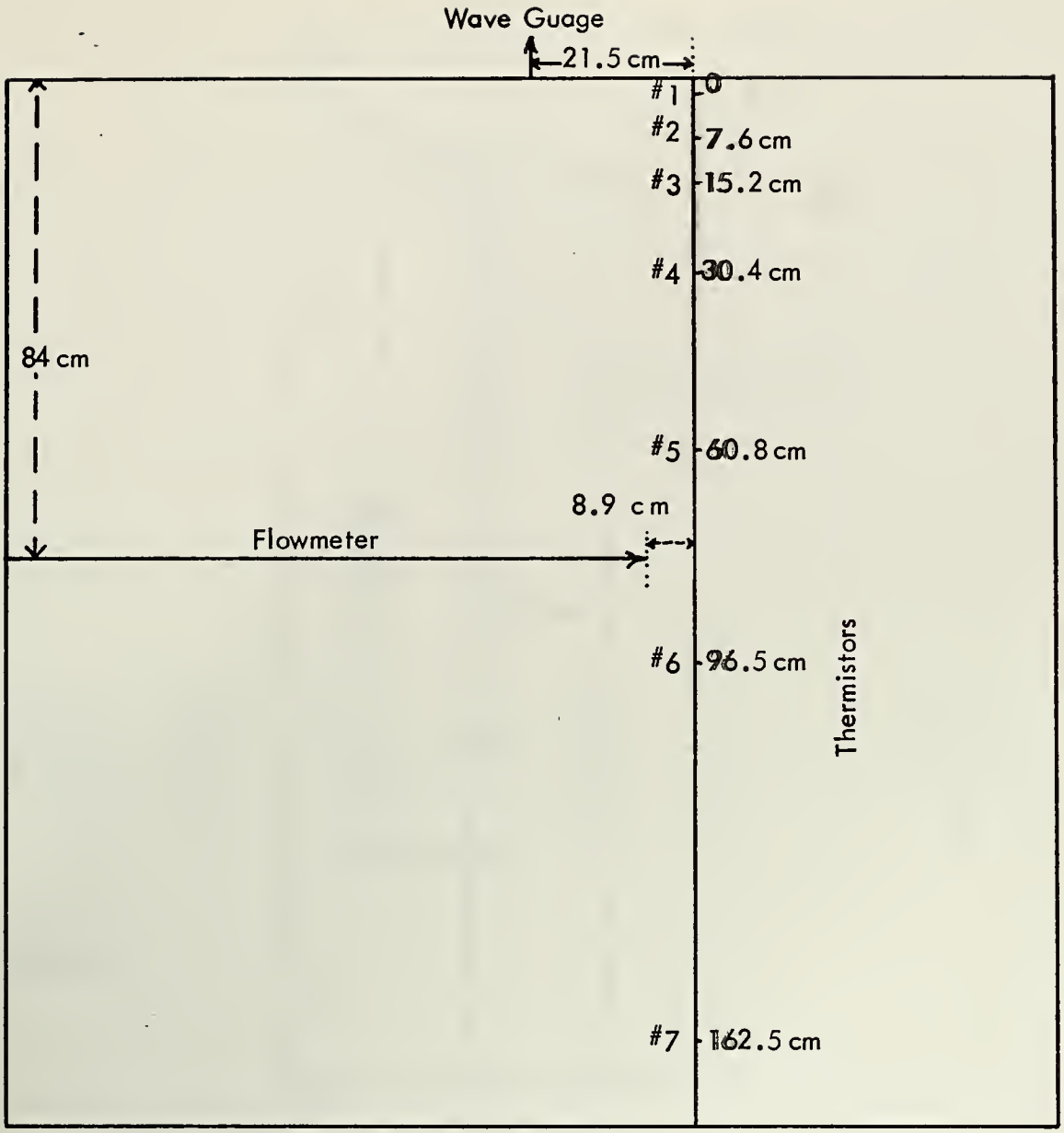

Figure 7. Configuration of Array for Runs One, Two, Three, and Four

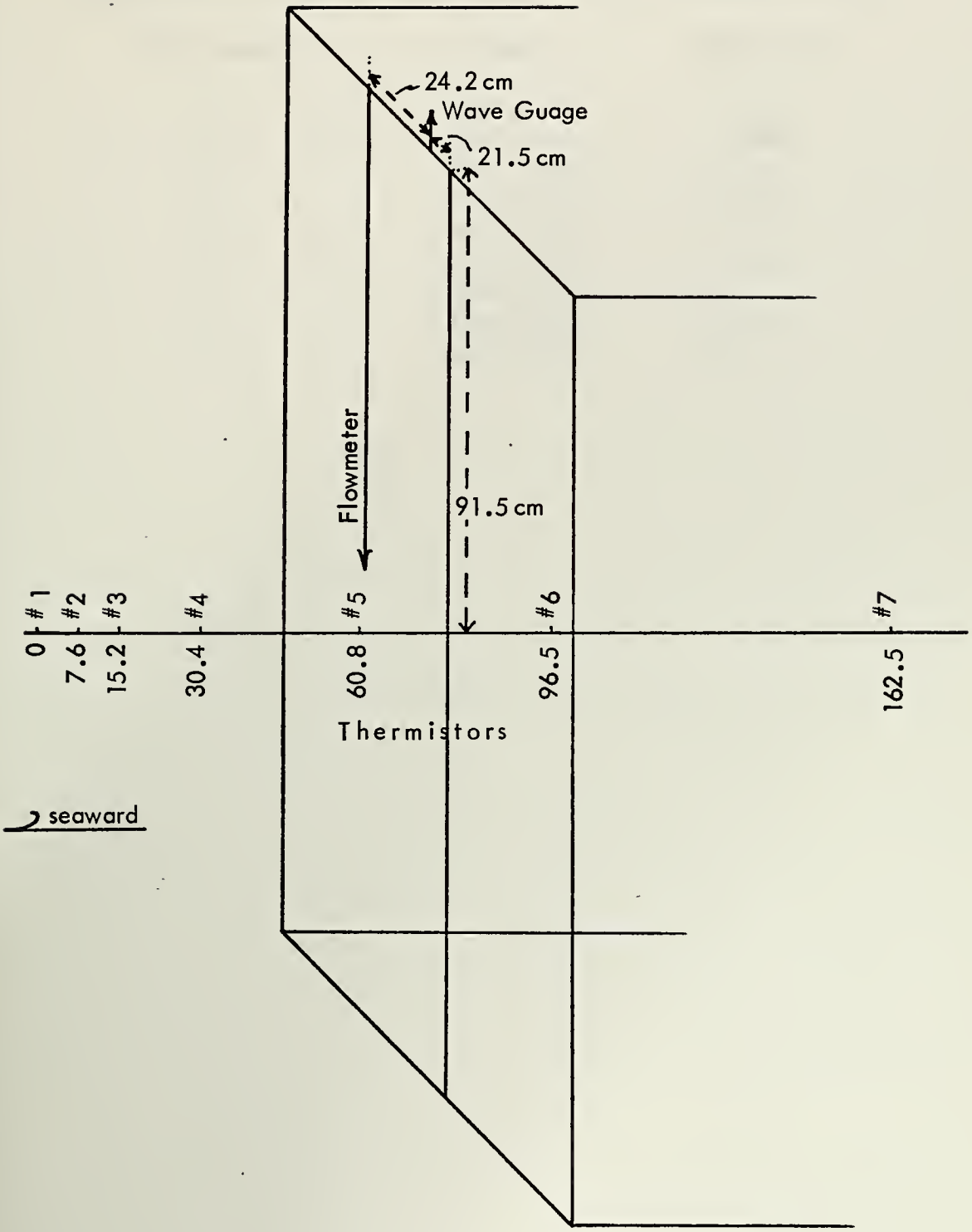

Figure 8. Configuration of Array for Run Six

Run times and depth of the top of the frame are given below:

Run number	Time	Depth (m)
1	1300-1340	2.7
2	1437-1510	5.2
3	1607-1640	11.3
4	1722-1755	2.7
5	1017-1034	2.7
6	1050-1201	2.7
7	1244-1315	8.5
8	1339-1400	13.1
9	1410-1430	13.1

III. DATA ANALYSIS

A. DATA PREPARATION

Analysis of the data was done at the Naval Postgraduate School. Initially all signals were graphically displayed on a strip chart for visual inspection, polarity checks, and checks for errors or anomalies. Immediately, two runs were discarded. Runs five and eight had been started with amplifier gains too high and too low and had overdriven and underdriven the tape recorder respectively. Runs six and nine had been made at the same depths and with the same configuration and therefore replaced five and eight. On runs seven and nine, there was a great deal of noise on the signal from the sixth thermistor; these runs were not analyzed.

Some long term fluctuations were noticed on all runs. Two runs showed significant internal wave activity. Run three showed a distinct internal wave in the top three thermistor traces (Fig. 9). Run six was started in the middle of an internal wave, spanned a second distinct wave, and included two patches of increased turbulence that may have been the remains of other internal waves (Figs. 10, 11).

Twenty minute portions of each run were chosen for analysis. This was the first 20 minutes in all but run six. In run six the portion for analysis did not include the large internal waves; the microstructure

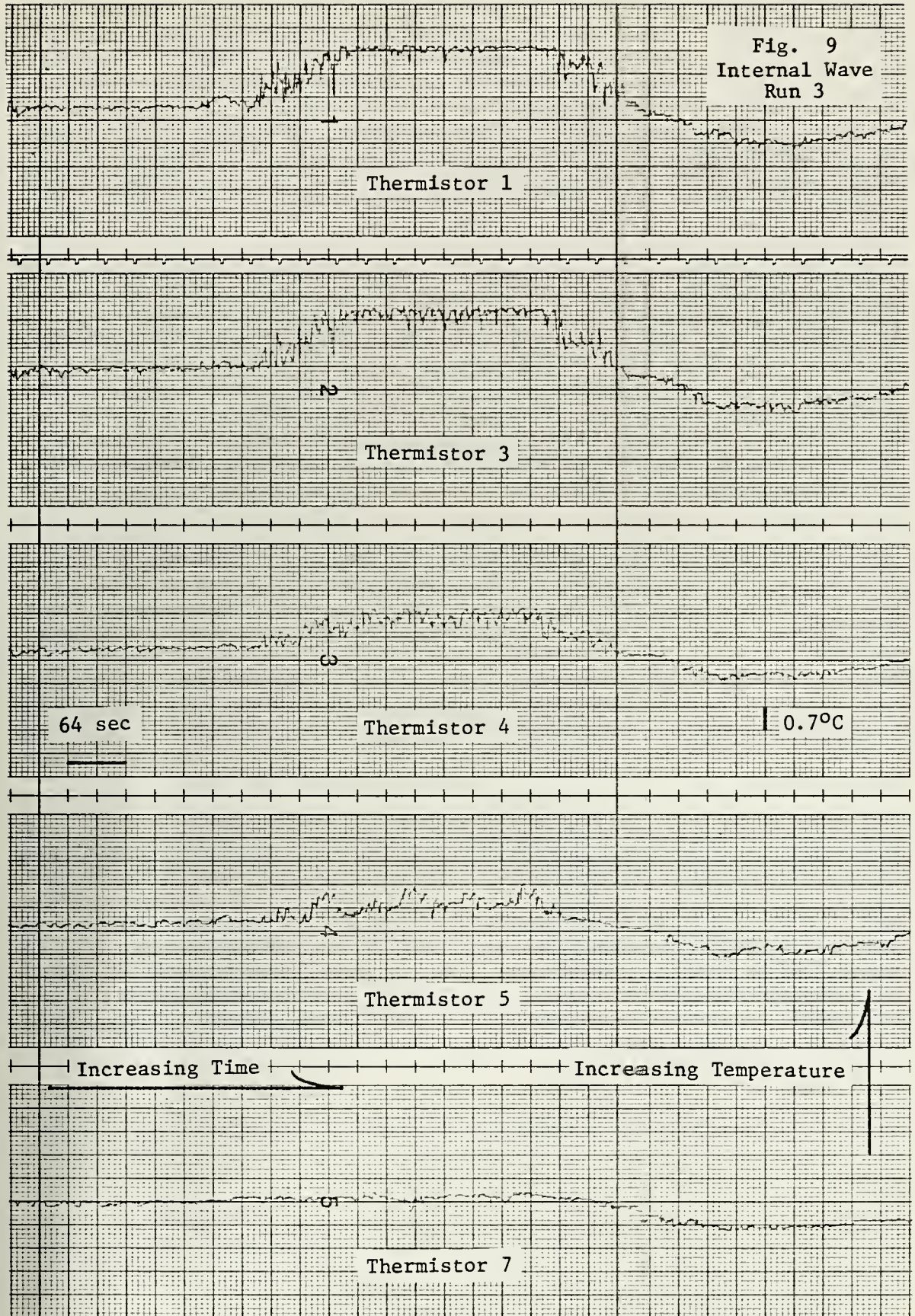
Fig. 9
Internal Wave
Run 3
Thermistor 1
Thermistor 3
Thermistor 4
64 sec
0.7°C
Thermistor 5
Increasing Time
Increasing Temperature
Thermistor 7

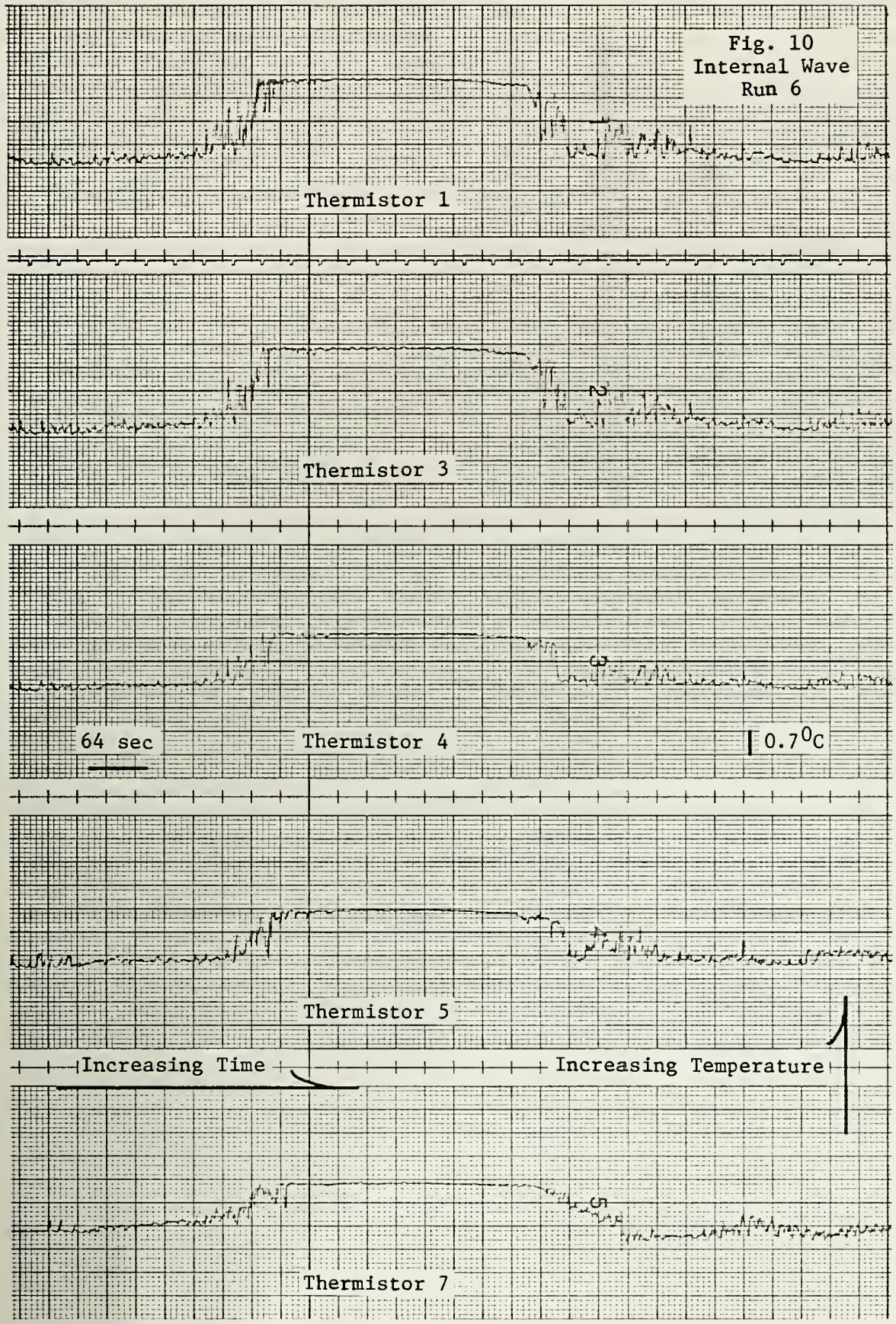
Fig. 10
Internal Wave
Run 6
Thermistor 1
Thermistor 3
Thermistor 4
64 sec
0.7°C
Thermistor 5
Increasing Time
Increasing Temperature
Thermistor 7

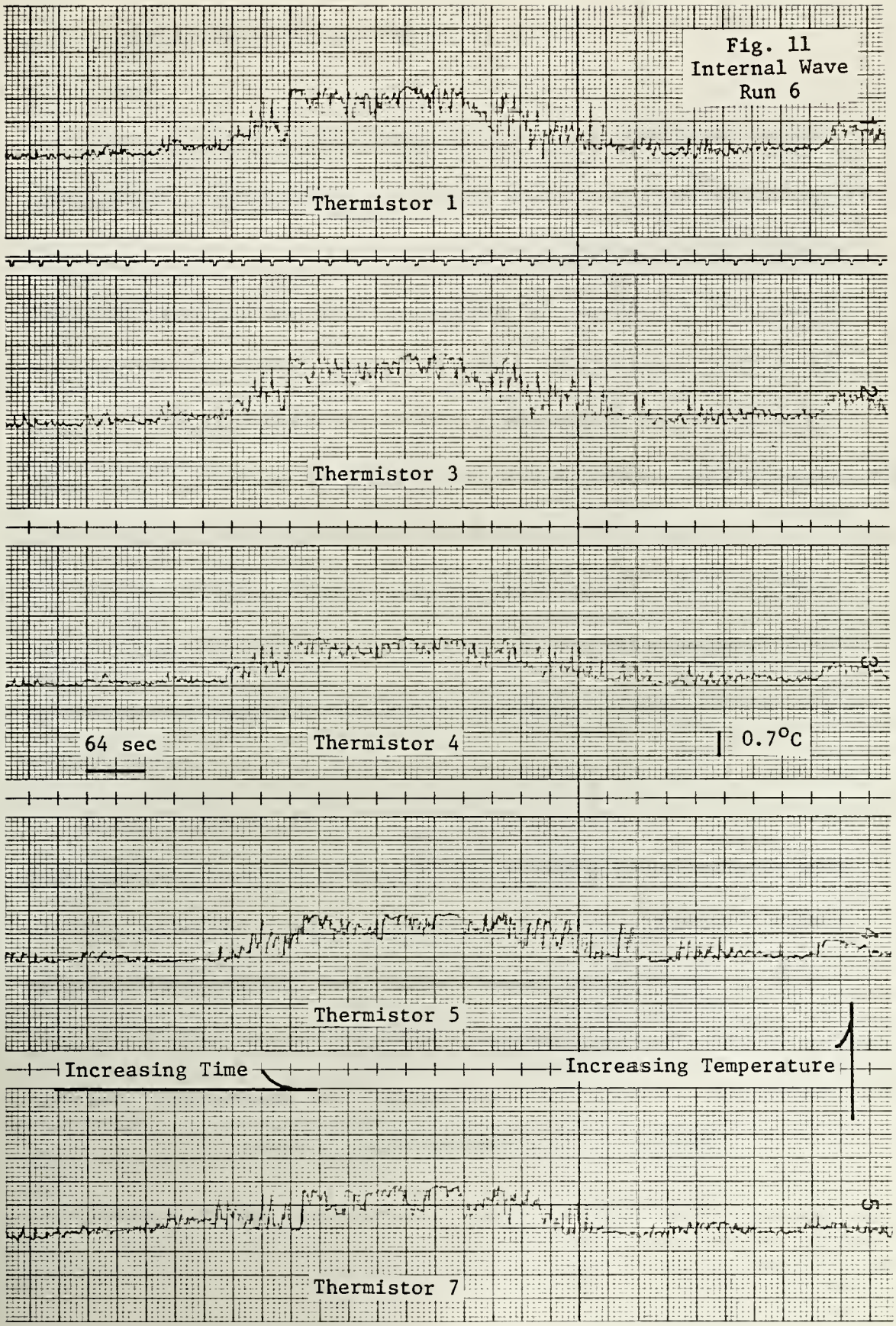

Fig. 11
Internal Wave
Run 6

in the internal waves did not appear to be representative of the rest of the run.

Once suitable portions of the data had been identified, they were digitized on a hybrid computer CI5000, XDS9300. Some runs required filtering of 60 Hz noise; this was done with Krohn-hite 3750 filters. Playback was at 60 ips with a sampling rate of 400 Hz, corresponding to a real time sampling rate of 12.5 Hz. The signals were further amplified during digitization to take advantage of the full dynamic range of the computer and thus increase resolution. Amplification was either x50 or x100 depending on the amount of fluctuation in the signal.

The seven track digital tape thus made on the hybrid computer was then transformed onto a nine track digital tape compatible with the school's IBM 360-67 computer on which the analysis was accomplished.

Since the scales to be analyzed were on the order of about one to 100 seconds, it was decided to filter out digitally any activity with a period of 100 seconds or greater. A Fourier analysis was made of each 20 minute segment of data; the coefficients were used to generate a time series describing the waves of period 100 seconds and greater. This series was then subtracted from the original time series. It was the filtered time series that was used for analysis.

The DC component and any trend were then deleted.

B. METHOD OF ANALYSIS

Temporal auto- and cross-correlations were computed for selected sensors. A Parzen window was first applied to the correlation functions. Auto- and cross-spectra were computed by a Fourier transformation on the correlation functions. Coherence and phase were computed from the cross-spectra. Due to the desire to cut down on computation time but keep the 20 minute record length, the number of data points was arbitrarily cut in half by deleting every other data point. This reduced the sampling rate to 6.25 Hz resulting in a Nyquist frequency of 3.1 Hz. The reduction in the Nyquist frequency was not considered critical, since the spectra became essentially flat and the signal lost in noise before the 3.1 Hz frequency was reached. Aliasing was experienced possibly from 60 Hz noise which was never effectively filtered out. The energy was always easy to identify, however, and appeared in narrow spikes at 2.59 Hz, and occasionally at 2.09, 1.04, and 0.67 Hz.

Spatial correlation was computed by averaging cross variance (C.V.) between the first thermistor (Th_1) and the others (Th_i), and normalizing with the variance of the first thermistor,

$$C.V. = \frac{1/T \int Th_1(t,x) Th_i(t, x+\Delta x_i)\, dt}{1/T \int (Th_i(t,x))^2\, dt} \quad , \quad i=1\text{-}7,$$

where T is the time over which the cross variance was computed

(20 min). The spatial correlation was then plotted against separation distance between thermistors using thermistor one as a reference; curve fitting was done by linear interpolation. The unnormalized spatial correlation functions were then transformed to obtain wave number power spectra in the same manner as described for the temporal functions.

IV. RESULTS OF THE ANALYSIS

A. TEMPORAL SCALES

One of the most common ways of presenting scales of inhomogeneities is to scale them by correlation times. In the present case, the correlation time is defined as the time required for the normalized autocorrelation function to fall to a value of 1/e (=0.368). In water with a constant temperature gradient (such as the mixed layer), it might be expected that the shortest correlation times would be at the surface where turbulence and short period waves dominate the structure. With increasing depth where turbulent mixing is not so intense and small scale temperature gradients have begun to smooth out, the correlation times should lengthen out to reflect the dominance of the surface wave motion. In the vicinity of a thermocline having internal waves, the times should again increase to reflect the dominance of the longer period internal waves, unless the internal waves are creating turbulence, in which case the correlation times can shorten again. In the shallow water of this experiment, turbulent mixing (and therefore shortening of the correlation times) may also have been caused by tidal currents. Consequently it is not surprising that the temporal correlations shown in table III show no dependence with depth.

In addition, the vertical dimensions of the thermistor array were small with respect to the extent of the water masses involved. The

TABLE III

CORRELATION TIMES & SIGNAL VARIANCES

Run 1			Run 2		
Thermistor	Time (sec)	Var ($^oC^2$) x10^{-5}	Thermistor	Time (sec)	Var ($^oC^2$) x10^{-5}
1	11.11	301	1	9.74	150
2	11.72	287	2	10.80	154
3	10.00	324	3	8.59	194
4	9.74	337	4	10.47	178
5	8.81	372	5	8.81	153
6	9.34	471	6	9.75	144
7	4.37	545	7	5.60	91

Run 3			Run 4		
Thermistor	Time (sec)	Var ($^oC^2$) x10^{-5}	Thermistor	Time (sec)	Var ($^oC^2$) x10^{-5}
1	3.28	950	1	14.40	115
2	4.10	1021	2	14.62	112
3	3.69	1230	3	12.88	52
4	3.89	1611	4	15.70	115
5	10.73	1722	5	17.26	74
6	5.40	1295	6	19.54	132
7	5.09	209	7	20.09	65

	Run 6	
Thermistor	Time (sec)	Var ($^oC^2$) x10^{-5}
1	3.35	5660
2	3.33	5674
3	3.16	5449
4	3.30	3129
5	3.95	4482
6	3.35	11519
7	4.60	4784

array therefore never really spanned the different temperature regimes adequately to draw any conclusions. However, as will be seen, the possible influence of turbulent mixing at the thermocline was noticeable on the traces of several thermistors on the edge of the array.

Runs one and two were made with the vertical thermistor array at the top of the thermocline (Fig. 12, 13). The bottom thermistor of each run shows a shorter correlation time than those above. This reflects the possibility that turbulence was being generated at the thermocline in the vicinity of the lower thermistors (Fig. 1). It is interesting to note in passing the apparently strong surface wave influence on the thermocline in run one as represented in the signal from the bottom thermistor, number seven. The upper thermistor shows almost no surface wave influence.

Run three, made in the thermocline, shows the most consistently short correlation times (Fig. 14) and tends to support the hypothesis that turbulence was being generated there. Discounting the correlation time for thermistor five which seems to be anomalously long, the two lower thermistors show longer correlation times than the others, indicating that perhaps the thermistor array extended below the thermocline outside of the active region. Run four, was made away from and above the thermocline and in nearly isothermal water (Fig. 15). It is the only one that shows long correlation times with respect to the other runs and shows a consistently increasing time with

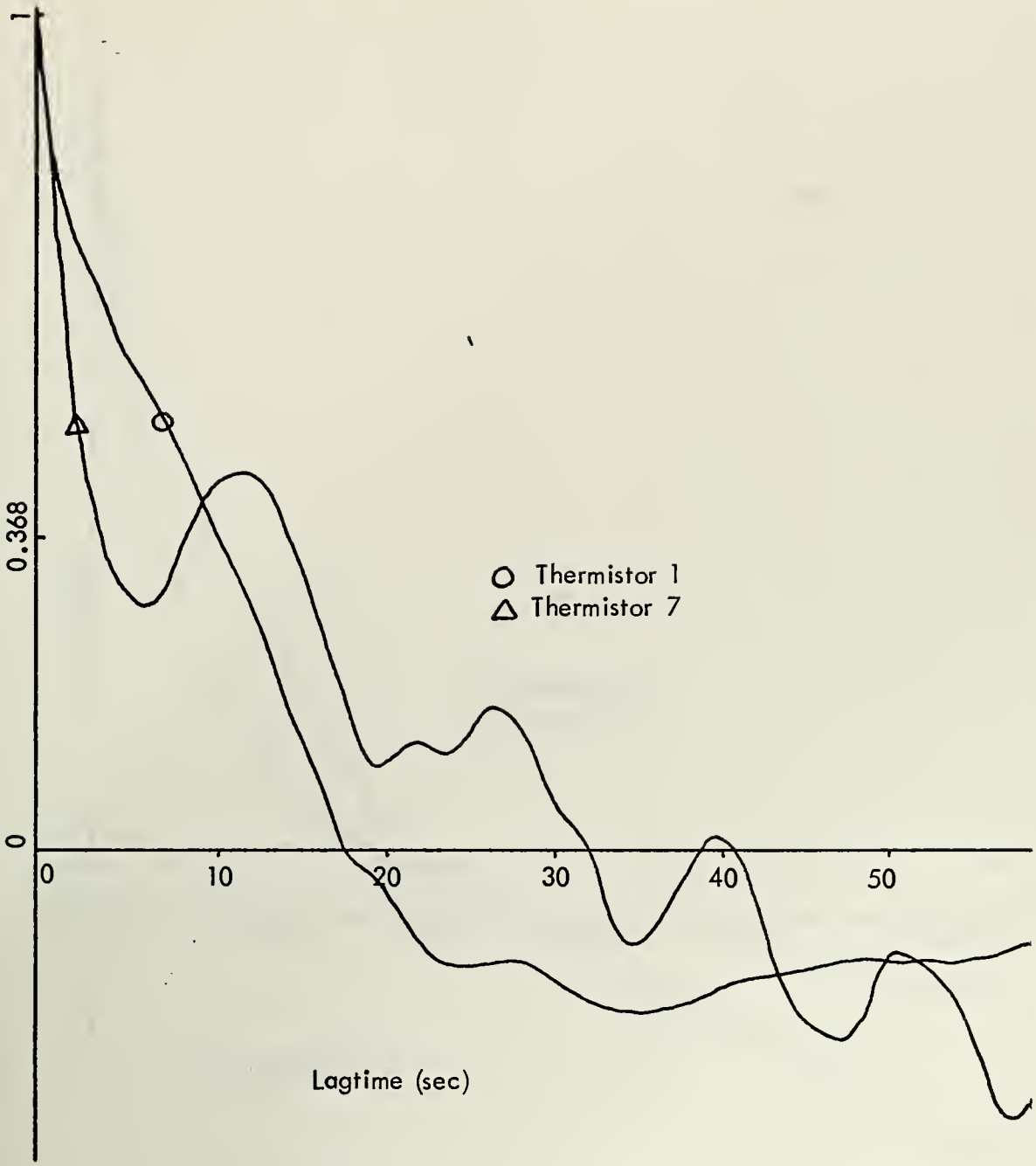

Figure 12. Autocorrelation Functions Thermistors One and Seven Run One

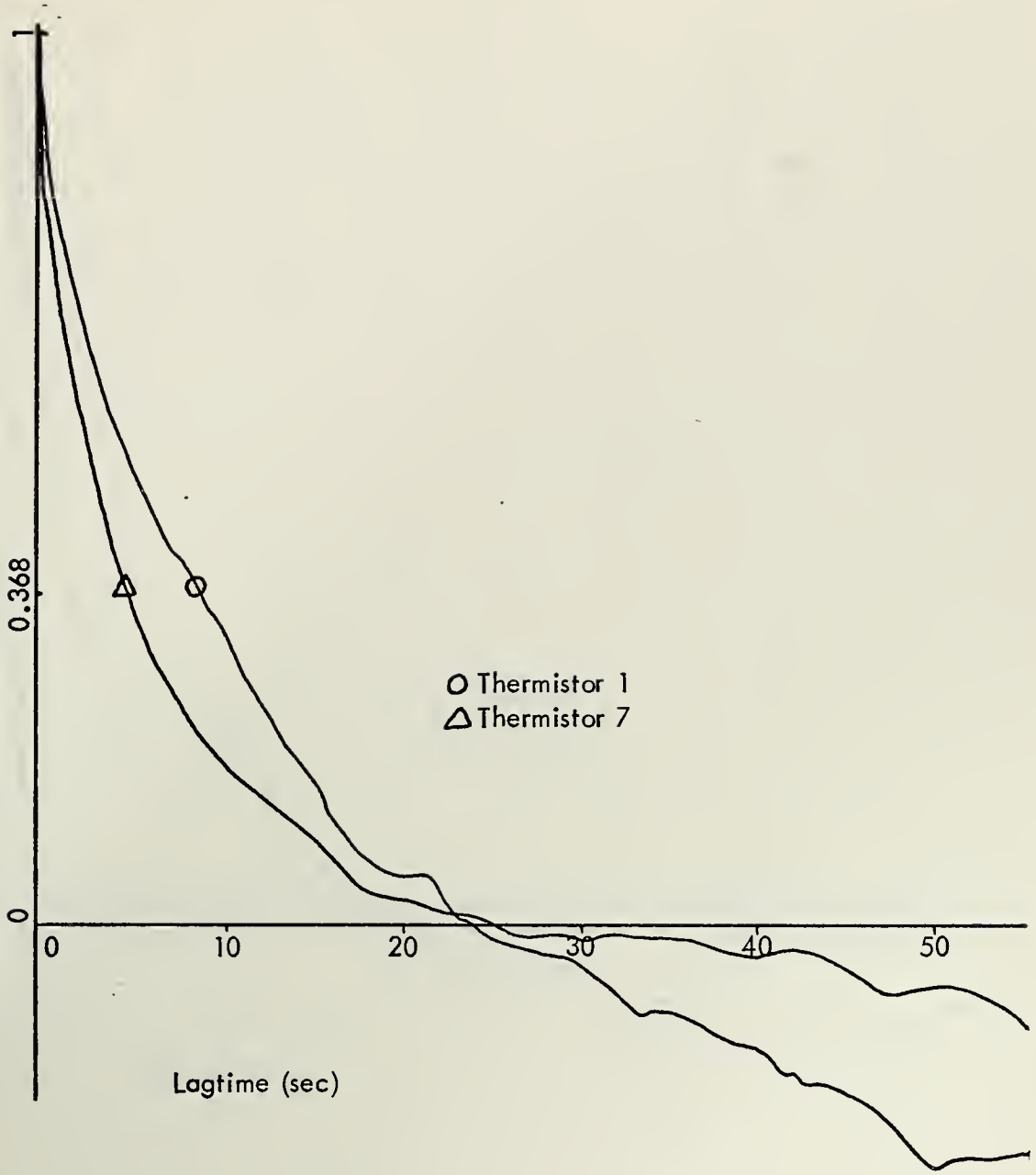

Figure 13. Autocorrelation Functions Thermistors One and Seven Run Two

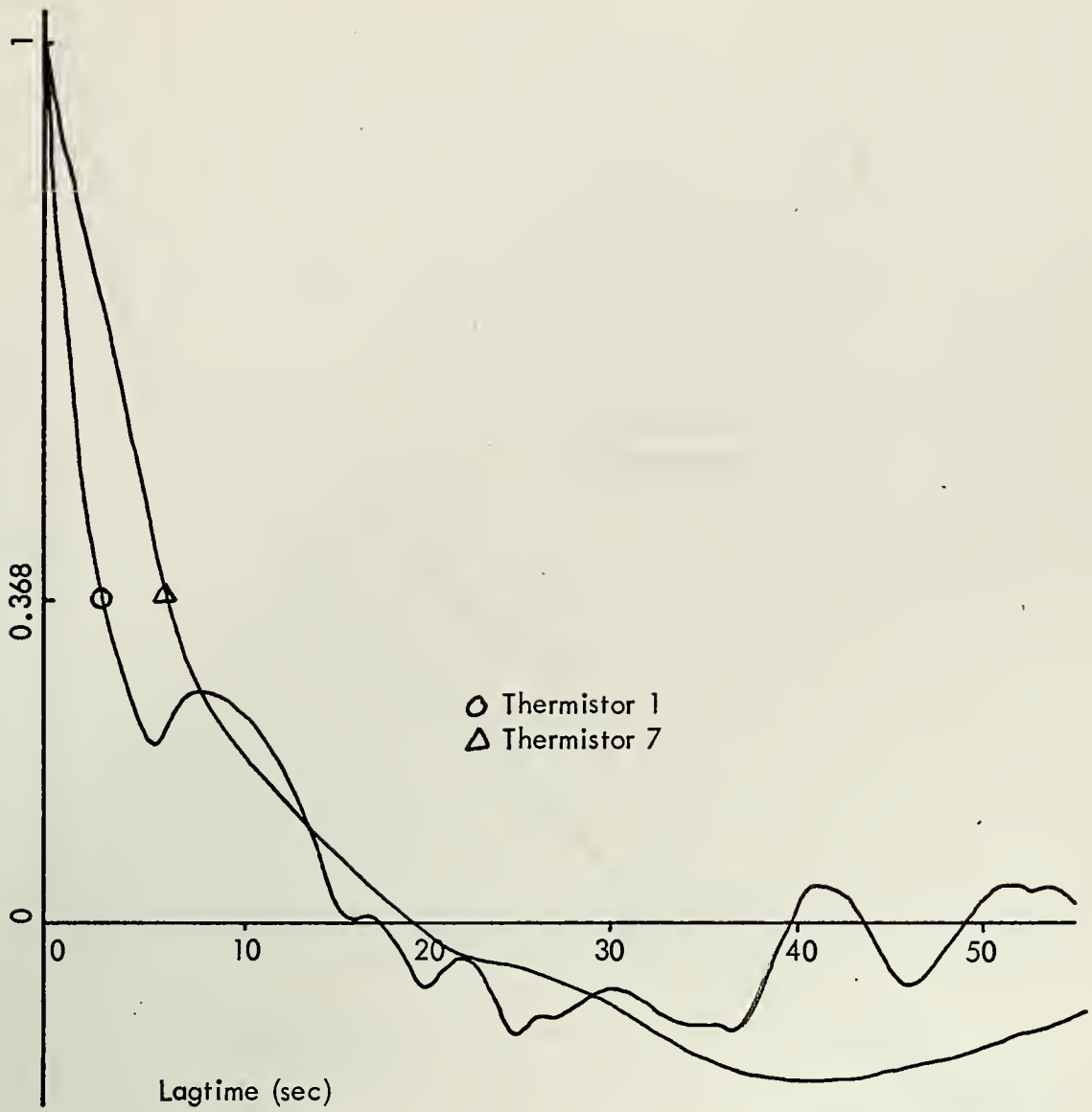

Figure 14. Autocorrelation Functions Thermistors One and Seven Run Three

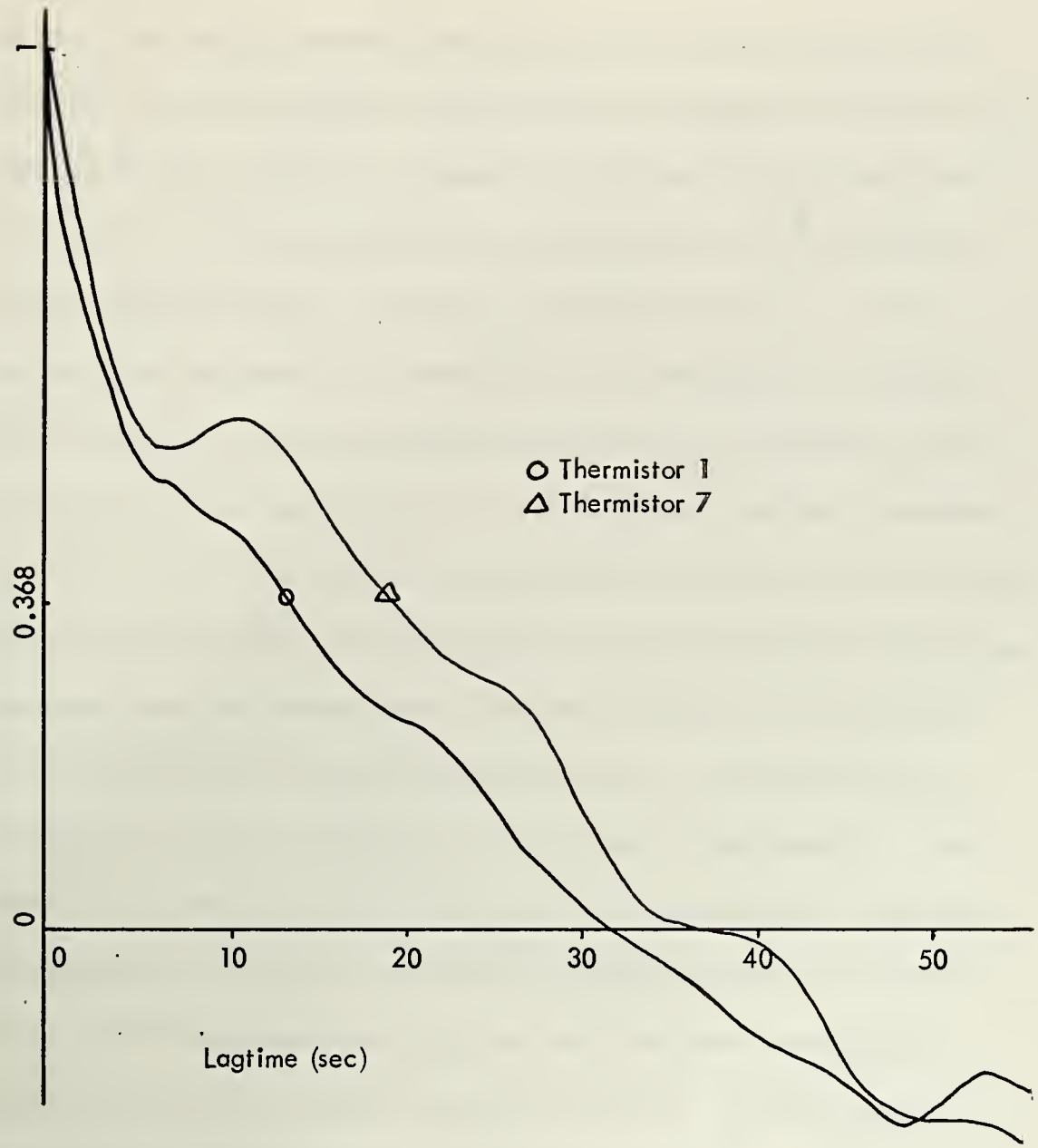

Figure 15. Autocorrelation Functions Thermistors One and Seven Run Four

depth. This large difference between the correlation times for runs four and the others implies that it is the distance from the thermocline that causes this difference. Supporting evidence for this interpretation comes from the fact that coherence between the wave gauge and the top thermistor of runs one and four is different (Fig. 16). For run one (and two and three) the coherence at the principal wave frequency never exceeds 0.24 implying that the surface waves had little influence on microstructure movement. For run four, the coherence increases to 0.48 at the wave frequency implying that the surface waves had more effect on the microstructure movement in nearly isothermal conditions removed from the thermocline. The wave spectra for runs one and four are very similar in power and shape (Fig. 17); the increase in coherence is therefore not due to an increase in wave activity. The peaks in the coherence are narrow and the spectral energy shown by the thermistors of this run is greater at frequencies lower than the surface wave frequency implying that there was still energy being supplied from sources other than surface waves. These results in general support the findings of Whittemore [1973].

If the edges of the thermocline are assumed to be areas of increased turbulence, then thermistors in that area should show not only a reduced correlation time but an increase in variance over those far from the thermocline. The results of the experiment are not conclusive in this respect (Table III). The variance of the bottom

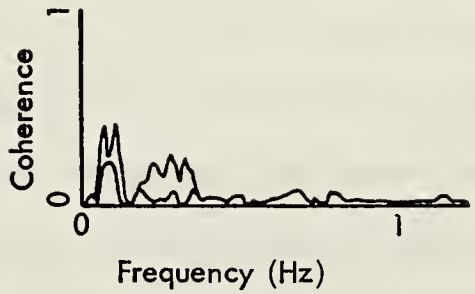

Figure 16

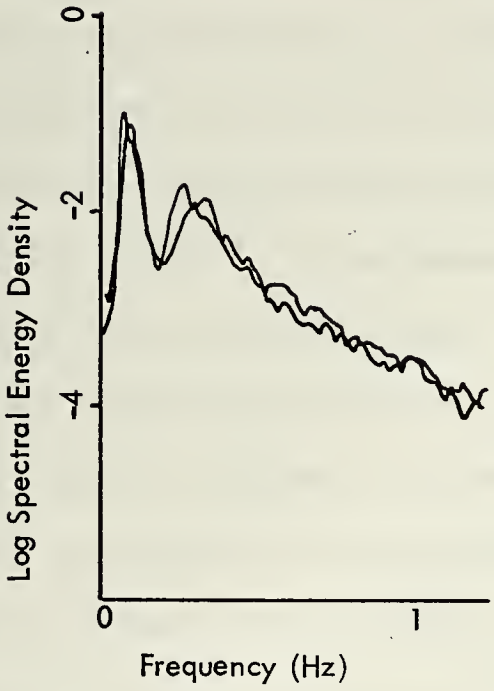

Figure 17

Comparison of Wave Spectra and Coherence
Between Wave and Thermistor One Spectra
Runs One and Four

thermistor for run one is nearly double that of the top thermistor ($545 \times 10^{-5}\ ^{o}C^{2}$ vs $301 \times 10^{-5}\ ^{o}C^{2}$) but for the second run it is smaller by nearly half ($91 \times 10^{-5}\ ^{o}C^{2}$ vs $150 \times 10^{-5}\ ^{o}C^{2}$). In run three, variances for the top six thermistors fall between $950 \times 10^{-5}\ ^{o}C^{2}$ and $1722 \times 10^{-5}\ ^{o}C^{2}$ but the bottom thermistor has a variance of only $209 \times 10^{-5}\ ^{o}C^{2}$. An order of magnitude range seems to be a very large range, but a visual inspection of the strip chart shows that the bottom thermistor may have been outside the influence of the thermocline and the area of greatest turbulent activity. All the variances for run three which was made within the thermocline, are at least a factor of three greater than those of the other runs indicating that mixing may have been more intense than in the other runs. Variances for run four do not follow any consistent pattern and vary between $65 \times 10^{-5}\ ^{o}C^{2}$ and $132 \times 10^{-5}\ ^{o}C^{2}$. No satisfactory explanation for this apparently random fluctuation could be found.

Auto-spectra for selected thermistors were plotted in order to determine if any power law relationships existed between turbulence and frequency; signals with such a relationship would show up as straight lines on log-log plots. The plots (Fig. 18) show a tendency toward constant slope in the frequency range 0.2-1.5 Hz, especially in the plot from run three thermistor one. The slopes are suggestive of turbulence in that the energy decreases with increasing frequency. However, the slopes are not consistent enough to support any generally

Figure 18. Autospectra for Temperature Signals, All Runs

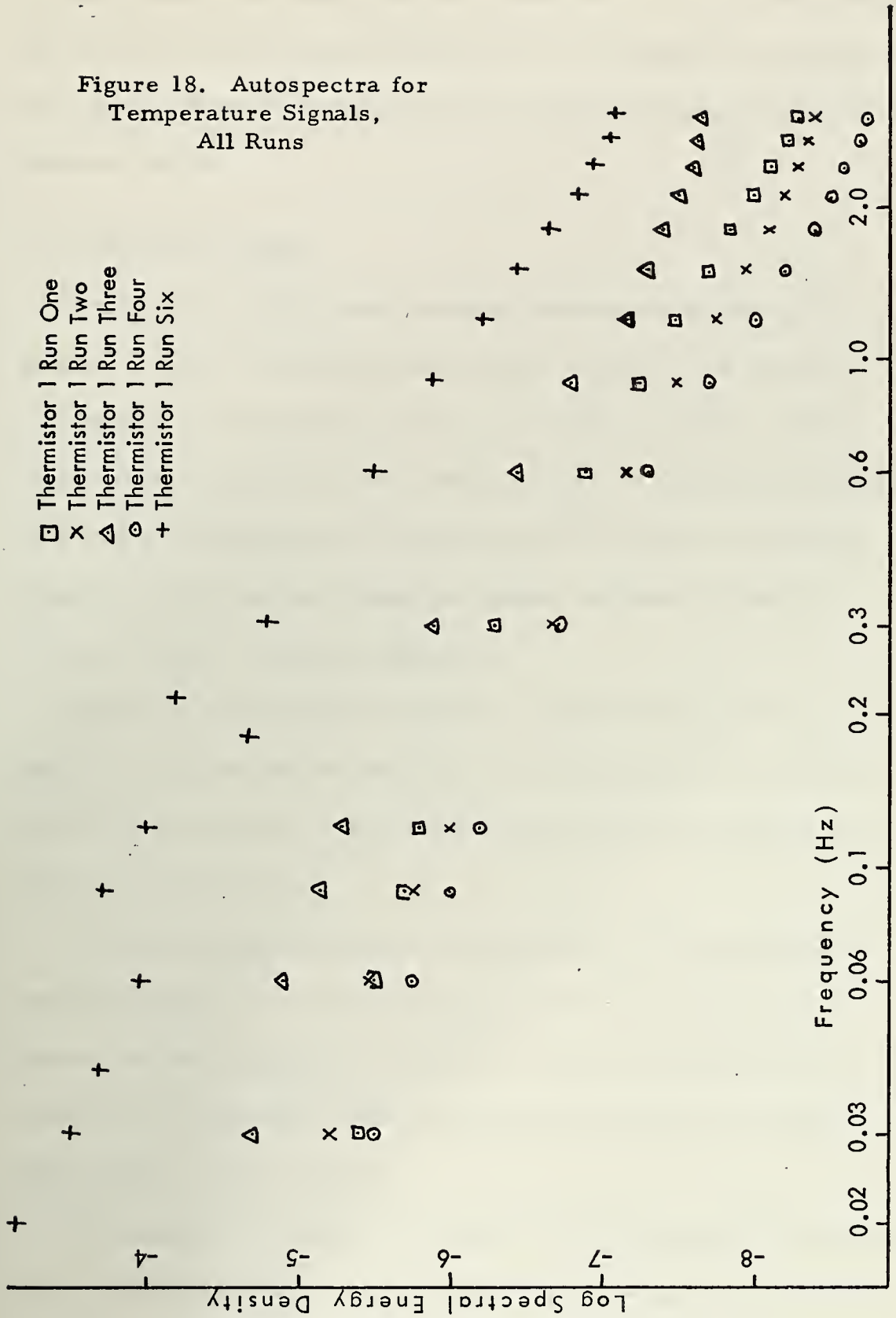

accepted power law theory such as Kolmogorov's inertial subrange law. The scales at which the data were taken were probably not sufficiently far removed from those of the internal waves to show purely turbulent characteristics.

B. SPATIAL SCALES

Thermistor signals were compared three ways in the spatial domain: spatial correlation, wave number spectra, and coherence.

Spatial correlations for runs one and two are similar, with correlation lengths of 102 cm, reflecting their same general relationship with the thermocline. Run three shows a shorter correlation length of 33 cm; run four shows the longest correlation length of 142 cm. Plots are shown in figure 19.

The runs (one and two) made at the edge of the thermocline have longer correlation lengths than that of run three which was entirely within the thermocline, but shorter than that of run four which was above the thermocline.

The wave number spectra are inconclusive. The spectrum for run one is figure 20. The energy from the very low wave number internal waves is apparently so great, even after filtering out the 100 second period waves, that energy leaks into the area of higher wave number surface waves.

For runs one through four and six, and for particular frequencies, coherency squared (or, simply, coherence) between thermistors was

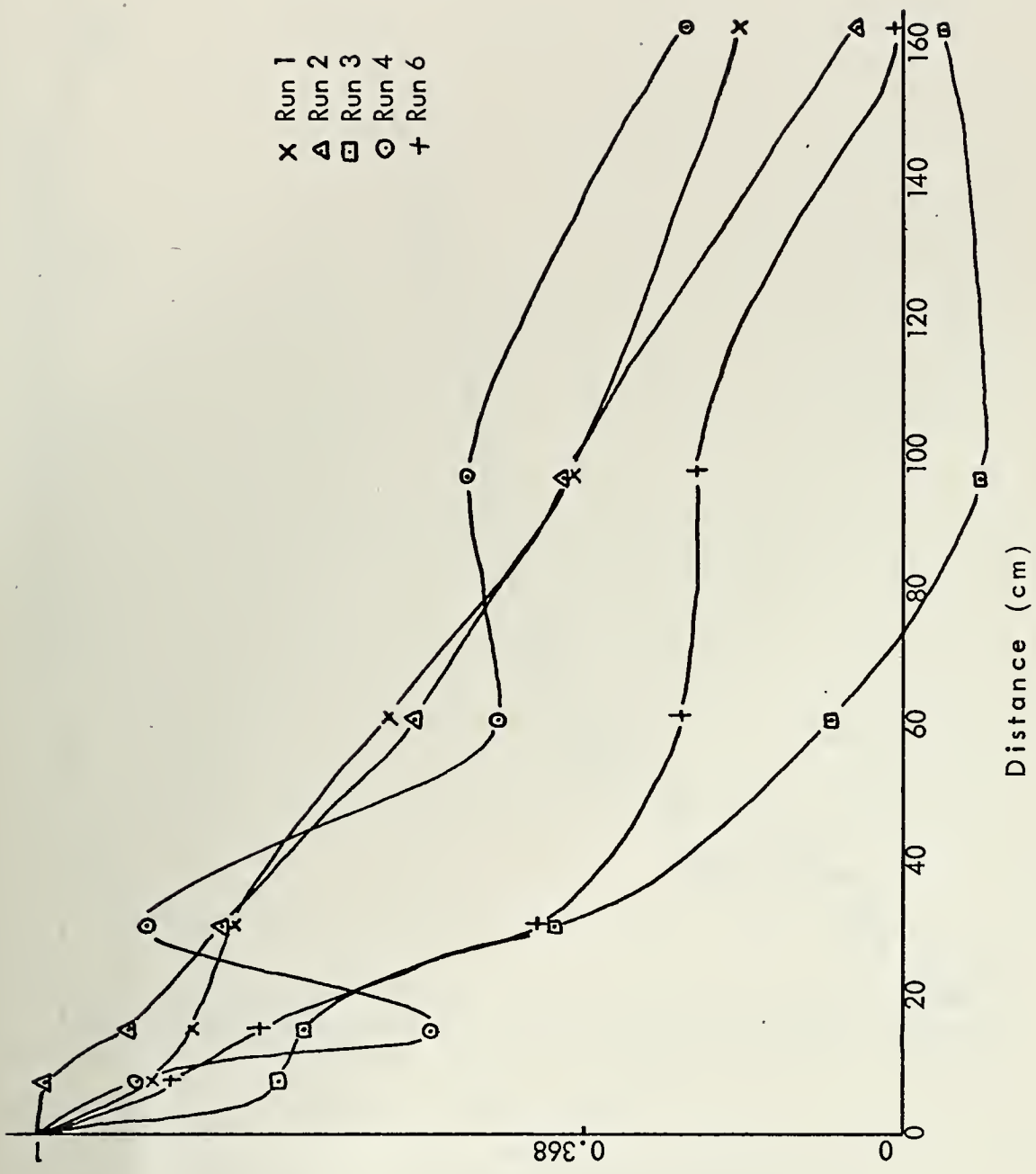

Figure 19. Spatial Correlations for Temperature Signals, All Runs

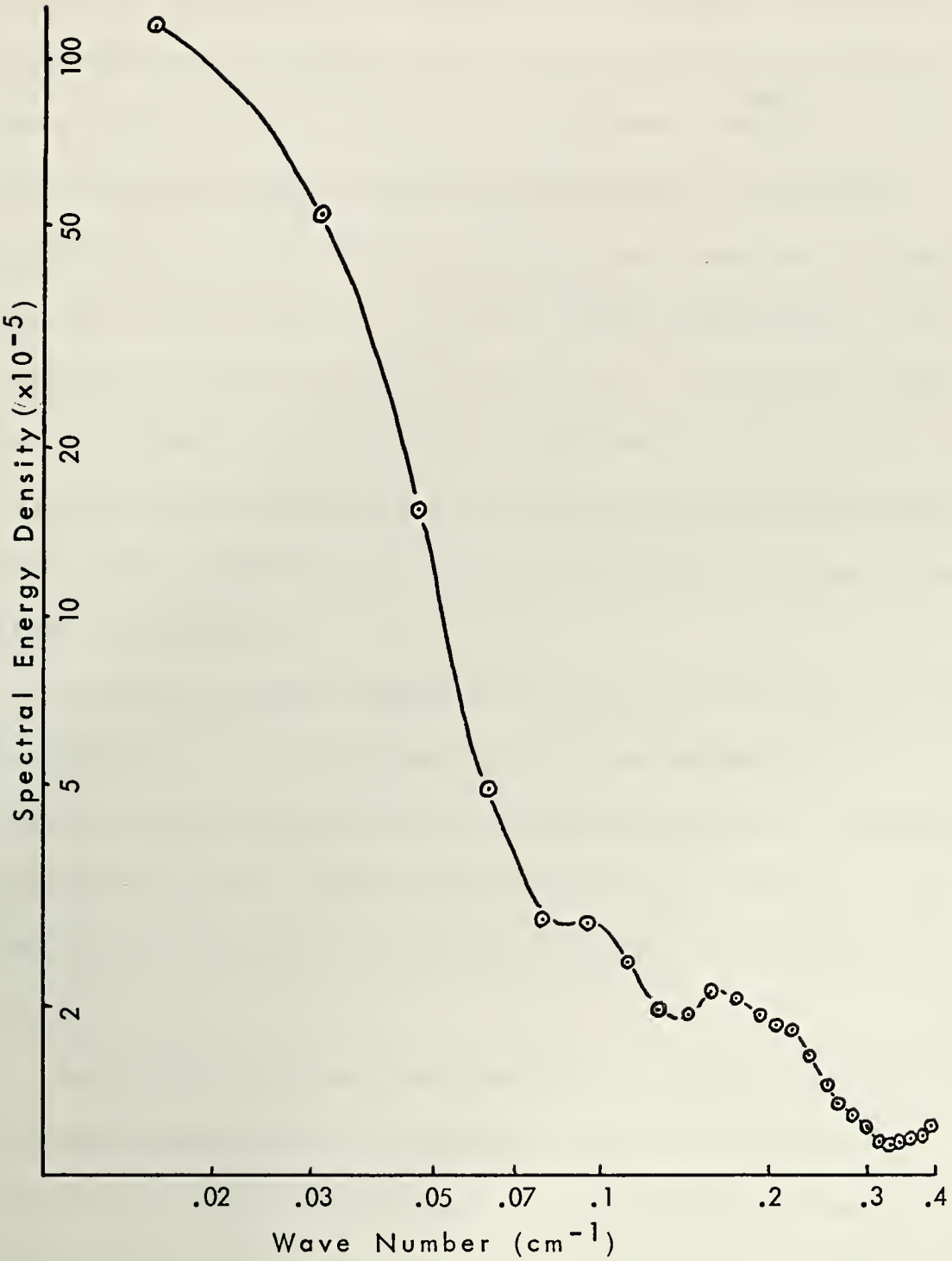

Figure 20. Wave Number Spectrum Run One

plotted against thermistor spacing using thermistor one as a reference. Figure 21 is for 0.008 Hz which may be considered as representative of the frequencies at which internal wave activity was found. Figure 22 is for 0.08 Hz where in general, maximum surface wave energy was found. Figure 23 is for 0.29 Hz, an arbitrarily picked high frequency. At the lowest frequency, coherence for runs one, two, and four falls to 1/e (0.368) in approximately 90 cm. The coherence in run three falls to 0.368 in 17 cm. It can be seen again that the random temperature fluctuations caused by the turbulence associated with the internal wave have a drastic effect in reducing the temperature field coherence as they did in reducing the temporal and spatial correlations.

At the surface wave frequency the picture is not so distinct. The run showing coherence of at least 0.368 for the longest distance is, as expected from previous discussion, run four at 38 cm. Runs one and two show 0.368 or better coherence to 15 cm. Run three, in the thermocline and subject to an internal wave, shows coherence out to 25 cm.

At the high frequency chosen, the spacing at which coherence remains greater than 1/e is expectedly short. Any turbulence present will dominate this frequency. In general the runs made in the presence of internal waves and the turbulence they cause show loss of coherence in shorter distances than those less affected by internal waves. Loss of coherence occurs between 5 and 10 cm.

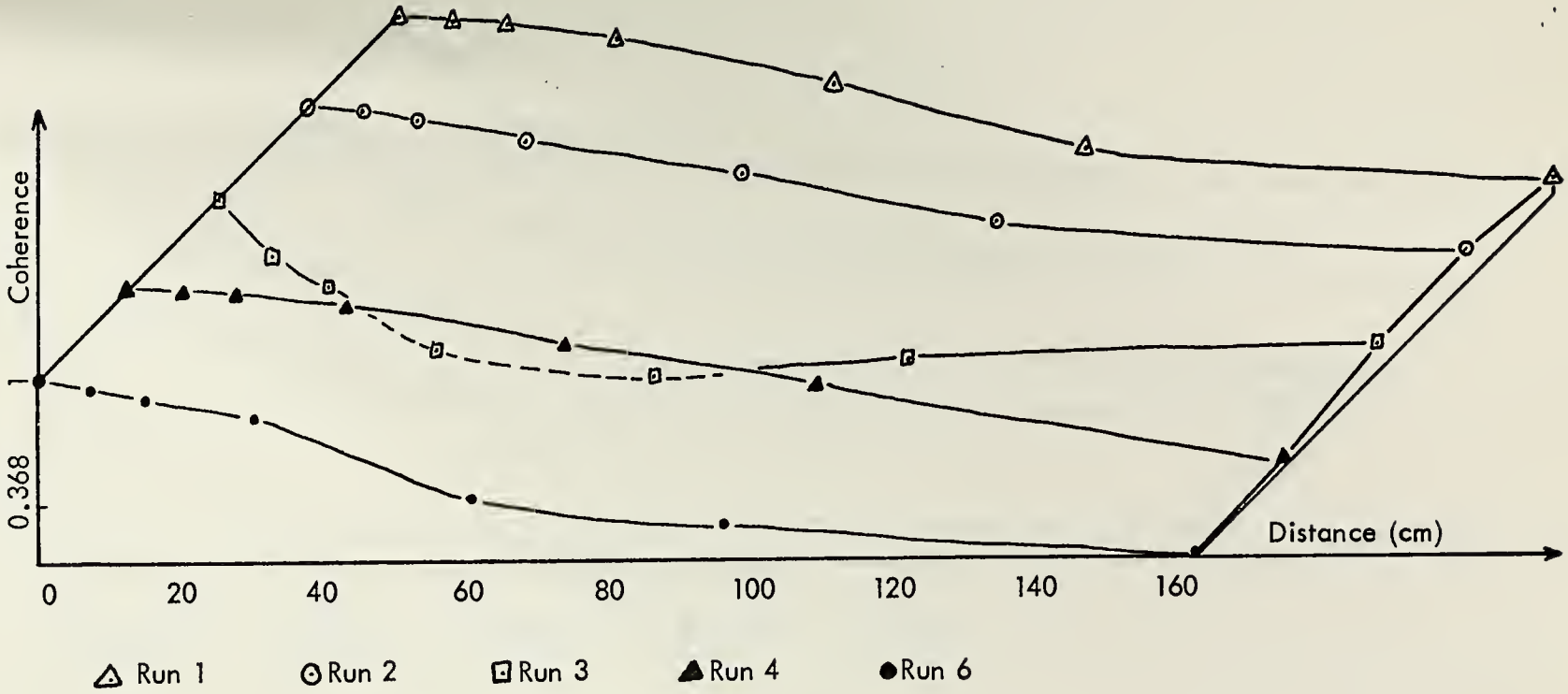

Figure 21. Temperature Signal Coherence as a Function of Thermistor Spacing: 0.008 Hz

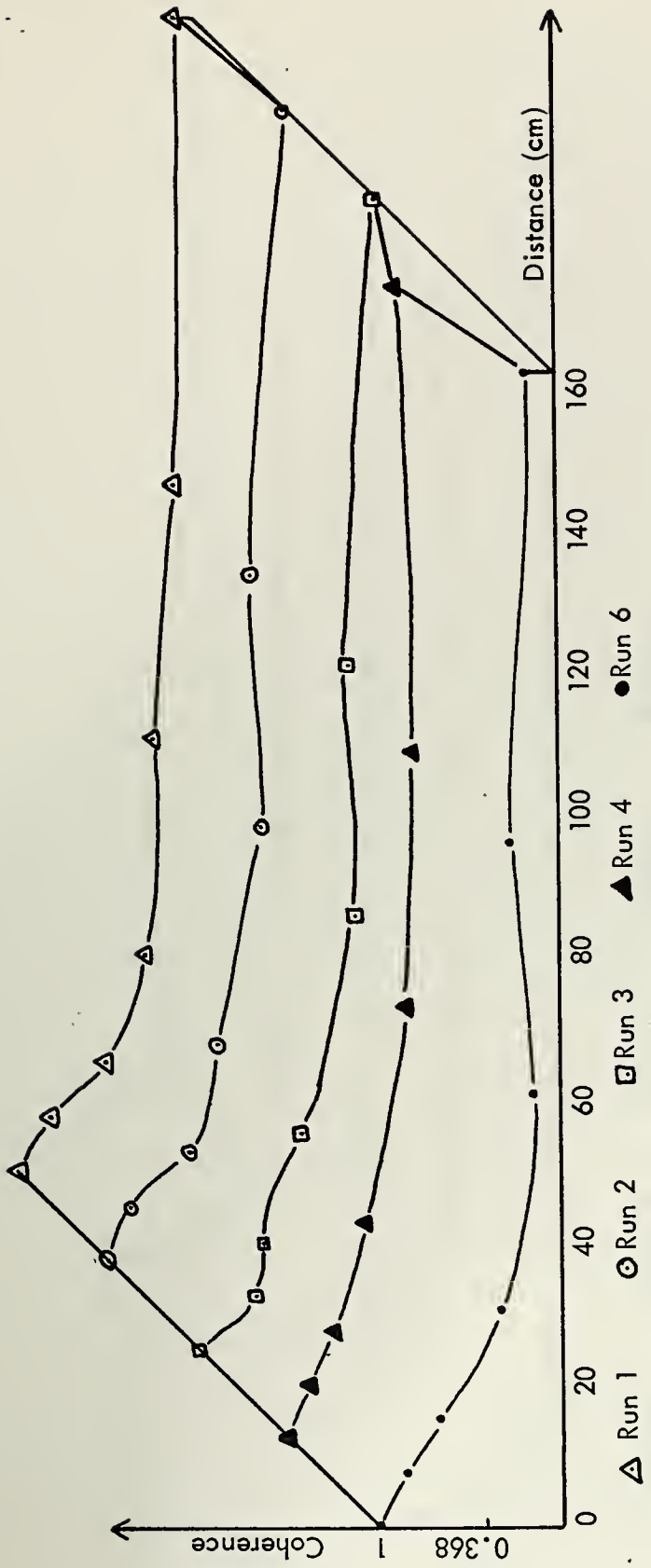

Figure 22. Temperature Signal Coherence as a Function of Thermistor Spacing: 0.08 Hz

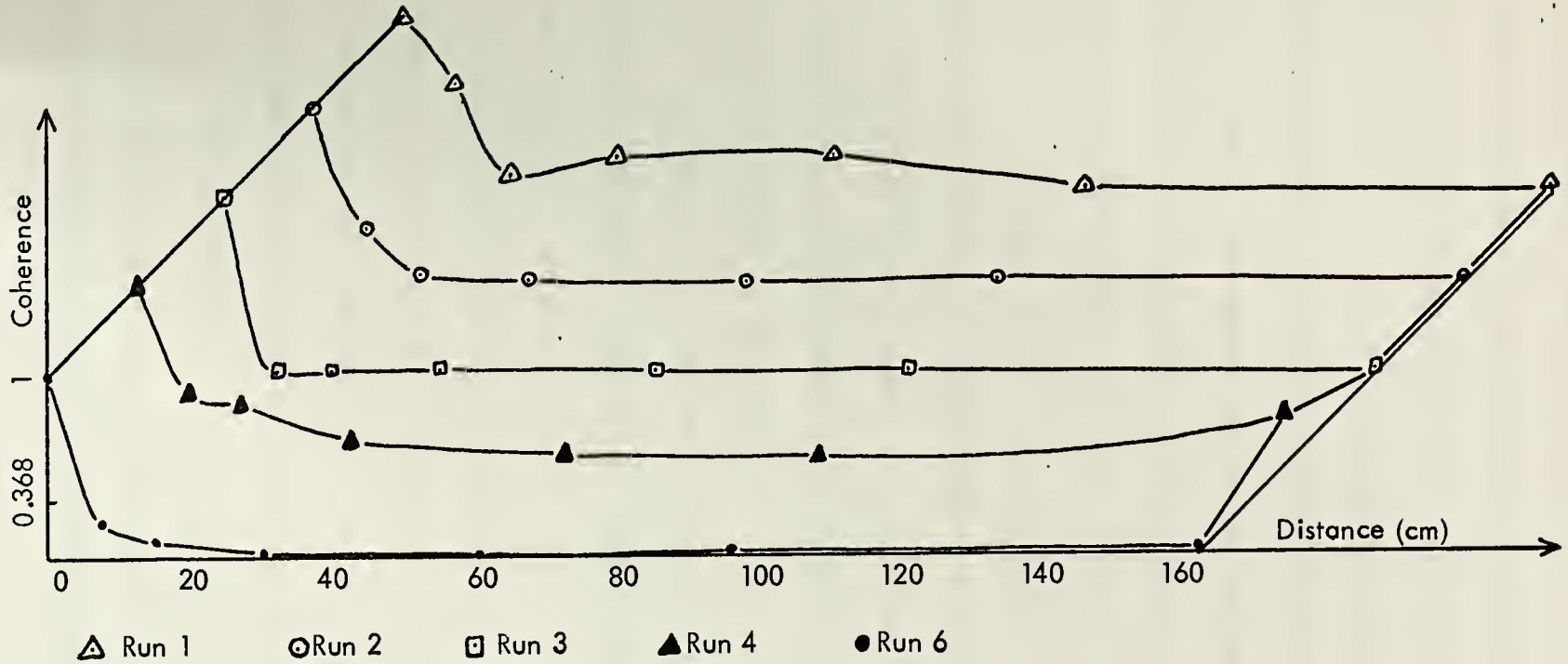

Figure 23. Temperature Signal Coherence as a Function of Thermistor Spacing: 0.29 Hz

C. COMPARISON OF THE VERTICAL AND HORIZONTAL SCALES

The relation between the vertical and horizontal scale sizes can best be seen through a comparison of run three vertical array and run six horizontal array, since both of these runs display a great deal of internal wave activity. It should be kept in mind for this comparison that the thermocline was more intense for run three than for run six ($0.79^{\circ}C/m$ vs $0.44^{\circ}C/m$); also, the upper part of the vertical array in run three was subject to internal waves whereas a visual inspection of the trace for run six reveals that all thermistors were affected by internal waves for that run. Nonetheless, since internal waves can be major contributors to turbulence, the comparison will be made.

A comparison of correlation times in table III shows that both runs have correlation times on the order of 3-4 sec. Variances for run six are, in general, consistent with each other, but they are about four times greater than those in run three. This may imply that mixing was more intense in run six.

Spatial correlations for the two runs are remarkably similar, both showing correlation lengths of about 38 cm (Fig. 24). The coherence for run six at the internal wave frequency (0.008 Hz) remains greater than 1/e over a much greater distance (58 cm) than for run three (17 cm) (Fig. 21). The implication is that internal waves are coherent over a longer distance horizontally than vertically. The coherence of the thermistors in run six at the surface wave

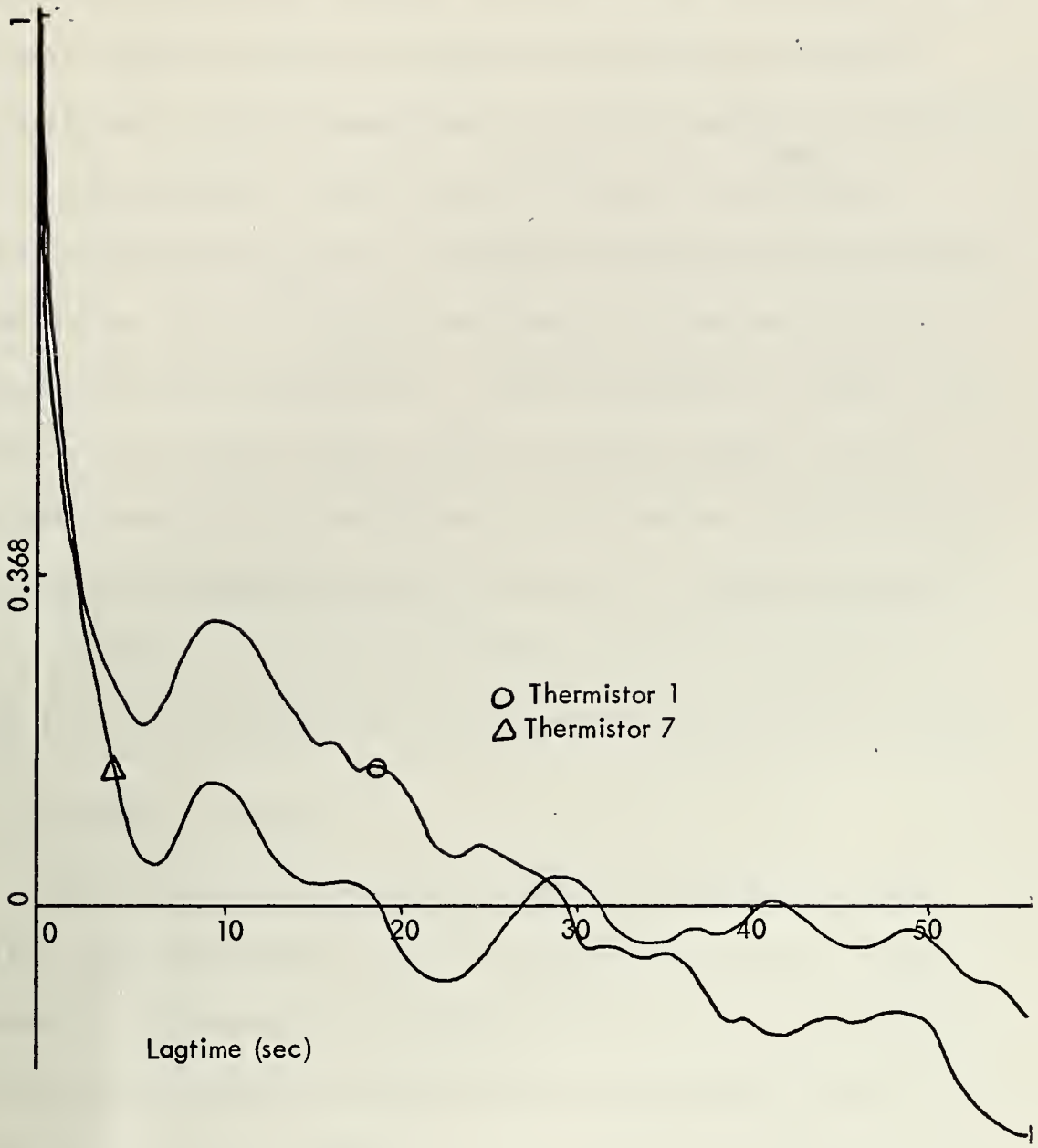

Figure 24. Autocorrelation Functions
Thermistors One and Seven Run Six

frequency falls off surprisingly fast with thermistor spacing. A plot of the coherence for the wave gauge and thermistor five (almost directly under the wave gauge) shows one of the highest values obtained at the principal wave energy frequency during the experiment (0.40 at 0.08 Hz) (Fig. 25). This implies that coherence between the thermistors should be high at that frequency. This does not occur, possibly because the thermistor spacing brackets the lengths of the surface wave particle orbits at which maximum coherence occurs. All that shows is a very small peak (0.26) at 96 cm. The coherence at 0.29 Hz is negligible and falls to 1/e at 5 cm. The fact that this value matches the value obtained from the runs with vertical arrays indicates the possibility of well developed turbulence at that frequency.

D. INTERNAL WAVES

Three aspects of internal waves could be seen from the data. First, when the thermistor array was vertical (run three), a wave passed which showed an instantaneous vertical picture of turbulence at the trough. Second, when the array was horizontal (run six), a trough passed giving a serial view of the wave energy being progressively degraded by turbulence. Third, also with the array horizontal (run six), the midpoint of an apparently large wave passed from which could be estimated the maximum probable dimensions of the wave and its phase speed.

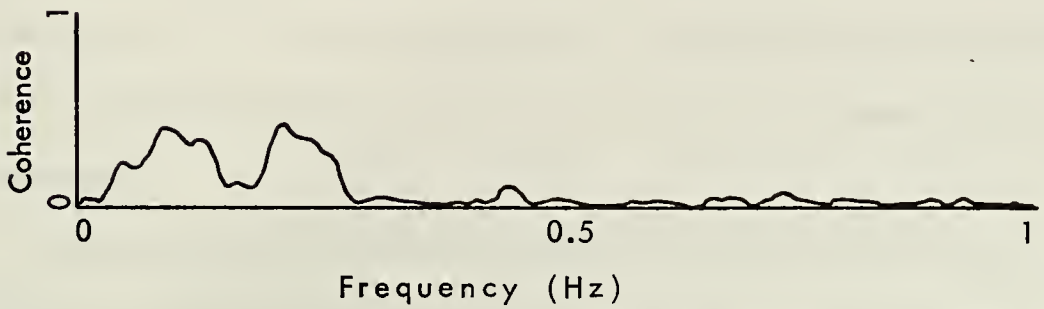

Figure 25. Coherence of Signals from
Wave Gauge and Thermistor Five Run Six

In the first case (Fig. 9) the temperature excursion across the wave is 2.7 °C corresponding to a wave height of 3.4 m assuming a constant temperature gradient of 0.79 °C/m. Since the wave appears distinctly only in the traces from the top three thermistors of the array and their total spacing is only 15.2 cm, there are not sufficient phase shifts to compute phase speed. The trace from thermistor five shows the internal wave breaking down into turbulence; four distinct eddies of amplitude 0.84 °C can be readily seen. The trace from thermistor seven shows the internal wave only just visible as a smooth diffuse undulation.

The second view of an internal wave creating turbulence is in figure 10. The trough of the wave apparently shows as it passes the horizontal array. In the trace from thermistor one, the warm sector has already been subject to some mixing with colder water and shows considerable structure. The trace from the seventh thermistor shows the warm sector nearly completely destroyed as an entity; instead a group of four well formed eddies has taken its place. Phase relationships show this change occurred in about 12 sec.

The third internal wave shown follows the one just discussed on the same run (Fig. 11). Since the array was horizontal, the thermistor traces again give a serial view of the wave passing. The traces are all similar in this case. The total temperature excursion of thermistor one as the wave passes is about 2.3 °C; this corresponds to a wave

height of 5 m assuming a temperature gradient of 0.44 °C/m in the thermocline. Phase relationships show a phase speed of 9 cm/sec. The warm sector is remarkably homogeneous and isothermal; temperature fluctuations are on the order of 0.14 °C whereas the fluctuations in the surrounding cold sections are on the order of 0.42 °C. This homogeneous warm water apparently comes from the surface mixed layer whereas the cold water comes from the vicinity of the thermocline where turbulence and microstructure are to be expected. The sudden onset and cutoff of intense temperature fluctuations (on the order of 1.4 °C in three seconds) on the boundaries of the wave are indicative of intense turbulent mixing. However, the mixing does not appear to be sufficiently advanced to have caused any degradation of the warm sector. This wave possibly is not subject to as intense a density gradient as the preceding wave due to the turbulent mixing caused by that preceding wave. BT casts were not made with sufficient frequency to show such short term fluctuations to determine this.

V. CONCLUSIONS

1. The temporal scales measured in the horizontal were greatly affected by turbulence. In the presence of turbulence, scales were of the order 4 seconds with a standard deviation of 0.8 seconds. Outside the influence of the internal waves scales were on the order of 10 seconds with a standard deviation of 4 seconds. In the presence of turbulence, correlation times were similar for both vertical and horizontal scales.

2. The spatial scales outside the influence of turbulence were of the order of 118 cm with a standard deviation of 21.5 cm. Under the influence of turbulence, they shortened to 33 cm. Vertical and horizontal scales in turbulent water were again similar.

3. The principal cause of turbulence appears to have been internal waves.

4. The data show the complexity of the temperature field off the NUC tower; they give some idea of the interplay between turbulence and internal waves during conditions of light winds, small waves and swell.

VI. RECOMMENDATIONS FOR FURTHER RESEARCH

1. It became apparent during this analysis that much firmer conclusions could have been drawn if more frequent BTs had been taken or a more continuous monitoring of the vertical temperature structure could have been made. A vertical thermistor array normally operating at the tower was not available during this experiment. Its use would have greatly aided interpretation of the data. Specifically, in some of the runs, events occurred at the top thermistors before the lower ones. This implies an internal wave cresting and beginning to break. Without the vertical profiles, this idea remains little more than speculation.

2. Current measurements at several depths would have given a measure of velocity shear and aided interpretations of the turbulent and internal wave fluctuations.

LIST OF REFERENCES

1. Alexander, C. H., Sound Phase and Amplitude Fluctuation in an Anisotropic Ocean, M.S. Thesis, Naval Postgraduate School, December 1972.

2. Bordy, M. W., Spectral Measurements of Water Particle Velocities Under Waves, M.S. Thesis, Naval Postgraduate School, March 1972.

3. Duchock, C. J., Jr., The Measurement and Correlation of Sound Velocity and Temperature Fluctuations Near the Sea Surface, M.S. Thesis, Naval Postgraduate School, March 1972.

4. Fitzgerald, James R., Statistical Study of Sound Speed in the Inhomogeneous Upper Ocean, M.S. Thesis, Naval Postgraduate School, December 1972.

5. Frigge, W. J., An Examination of the Salinity Sensing Capabilities of the STD Model 9006, M.S. Thesis, Naval Postgraduate School, March 1973.

6. Gossner, John, Comparison of Measured and Calculated Sound Velocity Near the Sea Surface, M.S. Thesis, Naval Postgraduate School, March 1973.

7. Haley, M. C., Small Scale Interaction in the Near Surface Ocean, M.S. Thesis, Naval Postgraduate School, December 1972.

8. Krapohl, R. F., Wave-Induced Water Particle Motion Measurements, M.S. Thesis, Naval Postgraduate School, December 1972.

9. LaFond, E. C., in M. N. Hill, ed, The Sea, Wiley Inter-Science, 1962.

10. LaFond, E. C., The U. S. Navy Electronics Laboratory's Oceanographic Research Tower, NEL Report 1342, 22 December 1965.

11. Phillips, O. M., The Dynamics of the Upper Ocean, Cambridge University Press, 1969.

12. Seymour, H. A., Jr., Statistical Relations Between Salinity, Temperature and Speed of Sound in the Upper Ocean, M.S. Thesis, Naval Postgraduate School, March 1972.

13. Shonting, D. H., and Kadis, A. L., The Thermiprobe: A System for Measuring Thermal Microstructure in the Sea, in F. Alt, ed, Marine Sciences Instrumentation, vol 4, Plenum Press, 1968.

14. Smith, W. J., Jr., Amplitude Modulation of an Acoustic Wave Propagating Near the Ocean Surface, M.S. Thesis, Naval Postgraduate School, December 1971.

15. Steer, R., Kinematics of Water Particle Motion Within Breaking Waves Within the Surf Zone, M.S. Thesis, Naval Postgraduate School, 1972.

16. Rautmann, J., Sound Dispersion and Phase Fluctuations in the Upper Ocean, M.S. Thesis, Naval Postgraduate School, December 1971.

17. Whittemore, M. A. N., Small Scale Temperature Fluctuations Near the Sea Surface, M.S. Thesis, Naval Postgraduate School, March 1973.

INITIAL DISTRIBUTION LIST

		No. Copies
1.	Defense Documentation Center Cameron Station Alexandria, Virginia 22314	2
2.	Library, Code 0212 Naval Postgraduate School Monterey, California 93940	2
3.	Department of Oceanography Naval Postgraduate School Monterey, California 93940	3
4.	Commander, Navy Ship Systems Command Code 901 Department of the Navy Washington, D. C. 20305	1
5.	Dr. Noel E. Boston, Code 58 Department of Oceanography Naval Postgraduate School Monterey, California 93940	38
6.	Dr. E. B. Thornton, Code 58 Department of Oceanography Naval Postgraduate School Monterey, California 93940	1
7.	Dr. Warren W. Denner, Code 58 Department of Oceanography Naval Postgraduate School Monterey, California 93940	1
8.	Professor H. Medwin, Code 61 Department of Physics Naval Postgraduate School Monterey, California 93940	1
9.	Dr. Ned A. Ostenso, Deputy Director (acting) Code 480D Ocean Science and Technology Division Office of Naval Research Arlington, Virginia 22217	1

10. Roberto Rodrigues,CDR, Brazilian Navy — 1
Instituto de Pesquisas da Marinha
1° Distrito Naval
Rio de Janeiro
Brasil

11. Dr. Robert E. Stevenson — 1
Scientific Liaison Office
Scripps Institution of Oceanography
La Jolla, California 92037

12. Oceanographer of the Navy — 1
Hoffman Building #2
2461 Eisenhower Avenue
Alexandria, Virginia 22217

13. Commander — 1
Naval Oceanographic Office
Washington, D. C. 20390
ATTN: Code 1640
ATTN: Code 70

14. NODC/NOAA — 1
Rockville, MD 20882

15. Director of Defense Research & Engineering — 1
Office of the Secretary of Defense
Washington, D. C. 20301
ATTN: Office, Assistant Director (Research)

16. Office of Naval Research — 1
Arlington, Virginia 22217
ATTN: Code 480
ATTN: Code 460
ATTN: Code 102-OS

17. Director — 1
Naval Research Laboratory
Washington, D. C. 20390
ATTN: Library, Code 2029 (ONRL)
ATTN: Library, Code 2620

18. Naval Oceanographic Office — 1
Library (Code 3330
Washington, D. C. 20373

SECURITY CLASSIFICATION OF THIS PAGE (When Date Entered)

REPORT DOCUMENTATION PAGE

READ INSTRUCTIONS BEFORE COMPLETING FORM

1. REPORT NUMBER	2. GOVT ACCESSION NO. / 3. RECIPIENT'S CATALOG NUMBER
4. TITLE (and Subtitle): A Study of the Effect of Internal Wave Induced Turbulence on Small Scale Temperature Structure in Shallow Water	5. TYPE OF REPORT & PERIOD COVERED: September 1973
	6. PERFORMING ORG. REPORT NUMBER
7. AUTHOR(s): Julian Edward Minard	8. CONTRACT OR GRANT NUMBER(s): Project Order No. P04-0121 ONR 55859 Research Project RR 131-03-01
9. PERFORMING ORGANIZATION NAME AND ADDRESS: Naval Postgraduate School Monterey, California 93940	10. PROGRAM ELEMENT, PROJECT, TASK AREA & WORK UNIT NUMBERS: Program Element 61153N Task NR 083-275-2
11. CONTROLLING OFFICE NAME AND ADDRESS: Naval Postgraduate School Monterey, California 93940	12. REPORT DATE: September 1973 13. NUMBER OF PAGES: 72
14. MONITORING AGENCY NAME & ADDRESS (if different from Controlling Office): Naval Postgraduate School Monterey, California 93940	15. SECURITY CLASS. (of this report): Unclassified 15a. DECLASSIFICATION/DOWNGRADING SCHEDULE

16. DISTRIBUTION STATEMENT (of this Report)

Approved for public release; distribution unlimited.

17. DISTRIBUTION STATEMENT (of the abstract entered in Block 20, if different from Report)

18. SUPPLEMENTARY NOTES

Master of Science Thesis supervised by Dr. N. Boston and Dr. E. Thornton, Associate Professors, NPS

19. KEY WORDS (Continue on reverse side if necessary and identify by block number)

Internal Waves
Turbulence
Thermocline
Small Scale Temperature Fluctuations

20. ABSTRACT (Continue on reverse side if necessary and identify by block number)

Measurements of temporal and spatial scale sizes of small scale temperature fluctuations were made in 19 meters of water from the NUC Oceanographic Research Tower off San Diego, California. Horizontal and vertical measurements were made using a two meter straight line array of seven thermistors. In addition to temperature, waves and orthogonal water particle velocities (turbulence) were measured simultaneously. Internal waves were found on two of five runs.

DD FORM 1 JAN 73 1473 (Page 1) EDITION OF 1 NOV 65 IS OBSOLETE S/N 0102-014-6601

20.

Average correlation length and time computed for the horizontal array runs without internal waves were 118 cm (standard deviation 21.5 cm) and 10 seconds (standard deviation 4 seconds). Measurements suggested that correlation obtained from the mixed layer were longer than those obtained at the edge of the thermocline. Internal wave induced turbulence reduced spatial and temporal scales to 33 cm and 4 seconds (standard deviation 0.7 seconds).

Vertical measurements taken in the presence of internal waves yielded spatial and temporal correlations of 38 cm and 4 seconds (standard deviation 0.7 seconds).